CHALMERS
UNIVERSITY OF TECHNOLOGY

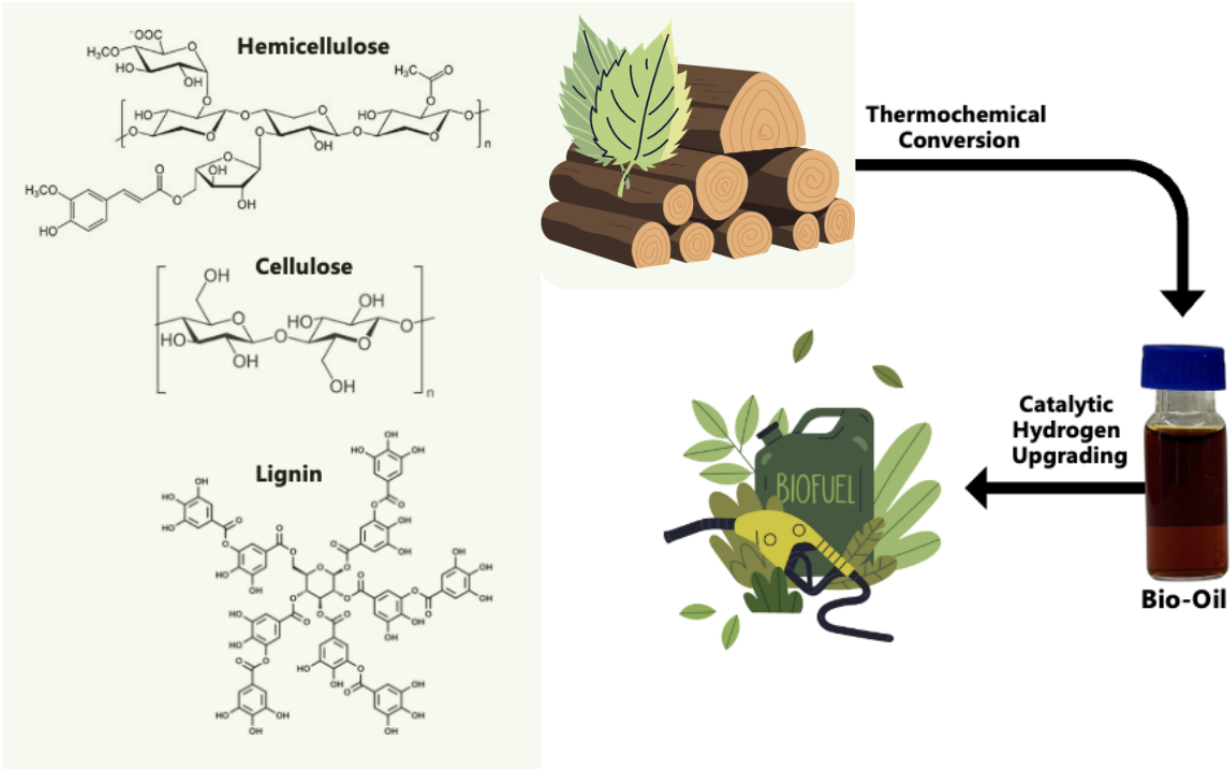

Analysis of the product compositions of hydrotreated bio-oils

Master's thesis in Materials Chemistry

SOFIE TRAPP

DEPARTMENT OF CHEMISTRY AND CHEMICAL ENGINEERING
CHALMERS UNIVERSITY OF TECHNOLOGY
Gothenburg, Sweden 2026
www.chalmers.se

Master's thesis 2026

Analysis of the product compositions of hydrotreated bio-oils

SOFIE TRAPP

CHALMERS
UNIVERSITY OF TECHNOLOGY

Department of Chemistry and Chemical Engineering
Chemical Engineering Division
Chalmers University of Technology
Gothenburg, Sweden 2026

Analysis of the product compositions of hydrotreated bio-oils
SOFIE TRAPP

Supervisors:
Johanna Rindebäck, VAROPreem
Olov Öhrman, VAROPreem

Examiner:
Louise Olsson, Chemical Engineering Division

Master's Thesis 2026
Department of Chemistry and Chemical Engineering
Chemical Engineering Division
Chalmers University of Technology
SE-412 96 Gothenburg
Telephone +46 31 772 1000

Cover: Conceptual overview of thermochemical conversion and catalytic hydrogen upgrading.

Typeset in LaTeX
Printed by Chalmers Reproservice
Gothenburg, Sweden 2026

Analysis of the product compositions of hydrotreated bio-oils
SOFIE TRAPP
Department of Chemistry and Chemical Engineering
Chalmers University of Technology

Abstract

Renewable feedstocks for fuel applications are of large interest due to the increasing urgency of reducing greenhouse gas (GHG) emissions and transitioning away from fossil fuels. Bio-oils derived from lignocellulosic biomass are promising renewable feedstocks for liquid fuel application, but their chemical instability, high oxygen content and low heating value are main limitations of such feedstocks. Therefore, direct refinery integration is not an option and catalytic hydrotreatment is a promising route for upgrading bio-oils to resemble conventional fuels and be used as drop-in fuel. This thesis investigates the hydrotreatment of pyrolysis oil (PO) and a novel forestry derived thermochemical bio-oil (BO) using Pd/C and $NiMo/Al_2O_3$ catalysts and oleic acid as a reference showcasing simple hydrodeoxygenation (HDO) chemistry. Liquid products were characterized by ^1H NMR for structural composition and GC-MS for molecular composition to evaluate compositional changes. Oleic acid underwent complete conversion over $NiMo/Al_2O_3$ under applied reaction conditions and showed a selectivity towards HDO, yielding the expected HVO100 chemistry, commercially used as drop-in fuel. For pyrolysis oil, a two step approach of stabilization under mild conditions followed by HDO resulted in an aliphatic hydrocarbon dominated product with a clear reduction of oxygenated species. The thermochemical bio-oil underwent a single step HDO treatment for the first time, producing a hydrocarbon rich product still containing oxygenates with various functional groups present. The results demonstrate that a stabilization step is essential for complex bio-oil feedstocks as the two step approach produced a more parafinnic, fuel-compatible product supporting the potential for bio-oil co-processing within existing refinery infrastructure. The work was conducted in collaboration with VARO-Preem, a leading energy company in Europe investing in renewable fuels with the aim of reducing the carbon footprint across the entire fuel value chain.

Keywords: Biofuels, Bio-oils, Hydrotreatment, Stabilization, Hydrodeoxygenation, Catalyst, Product Composition, Liquid Product

Acknowledgements

I would like to thank my supervisors Johanna and Olov from VAROPreem and my examiner Louise for continuously guiding me through this project with valuable discussions and constructive feedback. Johanna and Olov, your expertise in renewable energy and fuel production has been of great value for my work. Louise, your support in navigating the department and connecting me with the right people in the lab has made this project easier. During our Friday meetings, I have received guidance and encouragement for experimental and writing phases, and that is very much appreciated.

I would also like to thank Huy Xuan Le, Prabin Dhakal and Elham Nejadmoghadam for practical assistance in the laboratory and for support with the hydrogen gas reactor and analytical instruments. Thank you being patient with me, the reactor and the GC-MS instrument.

Lastly, and most important, I want to thank my family for supporting me through this hectic spring term as an elite athlete and full time student, and for always believing in me.

Sofie Trapp, Gothenburg, June 2026

List of Acronyms

Below is the list of acronyms that have been used throughout this thesis listed in alphabetical order:

BO	Bio-Oil
C12	Dodecane
C16	Hexadecane
C17	Heptadecane
C18	Octadecane
C18:1	Oleic Acid
$CDCl_3$	Deuterated Chloroform
DMDS	Dimethyl Disulfide
DMSO	Dimethyl Sulfoxide
FID	Flame Ionizing Detector
GC-MS	Gas Chromatography-Mass Spectroscopy
GHG	Greenhouse Gas
GPC	Gel Permatography Chromatography
HDO	Hydrodeoxygenation
HHV	Higher Heating Value
HTL	Hydrothermal Liquefaction
HVO	Hydrotreated Vegetable Oil
IPA	Isopropanol
NMR	Nuclear Magnetic Resonance
OA	Oleic Acid
PO	Pyrolysis Oil
TAN	Total Acid Number
TGA	Thermogravimetric Analysis

Contents

List of Acronyms **ix**

List of Figures **xiii**

List of Tables **xv**

1 Introduction **1**
1.1 Background . . . 1
1.2 Aim . . . 3
1.3 Limitations . . . 3
1.4 Outline . . . 4

2 Theory **5**
2.1 Bio-oils: Origin, Composition & Challenges . . . 5
2.1.1 Production Pathways . . . 5
2.1.2 Chemical Composition & Physical Properties . . . 6
2.2 Fatty Acids . . . 7
2.3 Catalytic Hydrotreatment . . . 8
2.3.1 Hydrodeoxygenation (HDO) . . . 10
2.4 Catalysts . . . 10
2.5 Analytical Methods . . . 11
2.5.1 Gas Chromatography-Mass Spectrometry . . . 11
2.5.2 Nuclear Magnetic Resonance . . . 12
2.5.3 Thermogravimetric Analysis . . . 12
2.5.4 Karl Fischer titration . . . 12

3 Methods **13**
3.1 Materials . . . 13
3.2 Catalyst Preparation . . . 13
3.2.1 Catalyst Activation . . . 14
3.3 Hydrotreatment Experiments . . . 14
3.3.1 Reactor Setup . . . 14
3.3.2 Stabilization and Hydrodeoxygenation . . . 15
3.3.3 Sample Collection . . . 16
3.4 Product Analysis . . . 17

4 Results & Discussion **19**

4.1 Oleic Acid as Reference 19
4.2 Physical Properties of the Bio-oils 20
4.3 Product Composition 22
4.3.1 Solid Product 22
4.3.2 Structural Composition by NMR 24
4.3.3 Molecular Composition by GC-MS 29

5 Conclusion & Future Outlooks **35**

Bibliography **39**

A Appendix A **I**

List of Figures

2.1 Reaction pathways for oleic acid during hydrotreatment, obtained based on information from [1]. 7
2.2 Hydrogenation reaction associated with catalytic hydrotreatment for bio-oil upgrading. Drawn on the basis of information from [2]. 9
2.3 Hydrogenation reaction associated with catalytic hydrotreatment for bio-oil upgrading. Drawn on the basis of information from [2, 3]. . . . 10

3.1 Procedure for collection of liquid samples, the glass filter collects the solid product while the liquid product proceeds through the filter. . . 16
3.2 Schematic overview of the experimental workflow, including the bio-oil feedstocks, hydrotreatment process, product separation and analytical techniques used. 17

4.1 GC-MS/FID chromatogram of the oleic acid feed and product with corresponding compounds visualized. 19
4.2 Physical appearance of the pyrolysis oil before, during and after the two-step hydrotreatment. 21
4.3 Physical appearance of the thermochemical bio-oil before and after HDO. 21
4.4 Comparison of hydrogen-treated bio-oil samples immediately after treatment and after one week of storage at room temperature. From the left: hexadecane phase, acetone phase. 22
4.5 Solid product yields after the first stages of the hydrotreatments applied to PO and BO respectively. 23
4.6 TGA of the bio-oils before hydrotreatment used to validate reaction conditions applied. 23
4.7 ^{1}H-NMR spectra of the pyrolysis oil, comparison between feedstock, mild stabilized product and HDO product. 25
4.8 Schematic illustration of aldehyde reduction to an alcohol during mild hydrotreatment, using the conversion of succindialdehyde to 1,4-butanediol as an example. 26
4.9 ^{1}H-NMR spectra of the pyrolysis oil, comparison between stabilized hexadecane phase and acetone fraction. 27
4.10 Schematic illustration of aldehyde hydrogenation to alcohol and subsequent hydrodeoxygenation to alkane. 28
4.11 ^{1}H-NMR spectra of the thermochemical bio-oil, comparison between feedstock dissolved in IPA and HDO product. 29

4.12 GCxGC-MS/FID data showing distribution of component classes present in the two bio-oils with classification based on identified compounds, and species with a library hit probability below 10% excluded. 30
4.13 GCxGC-MS/FID product composition after hydrotreatment of the pyrolysis oil, showing the distribution of hydrocarbon and oxygenate compound classes as volume percentage, and species with a library hit probability below 10% are excluded. 31
4.14 GCxGC-MS/FID product composition after hydrotreatment of BO, showing the distribution of hydrocarbon and oxygenate compound classes as volume percentage, and species with a library hit probability below 10% are excluded. 32

List of Tables

3.1 Reaction conditions for the activating processes of the catalysts used for hydrotreatments. 14
3.2 Reaction conditions, catalysts and oil loadings used for hydrotreatment of the bio-oils. 15

4.1 Product selectivity for oleic acid HDO over $NiMo/Al_2O_3$ (325 °C, 30 bar H_2). 20

A.1 GC-MS chromatograms of the PO feedstock, showing the identified compounds along with their names and chemical formulas. I
A.2 GC-MS chromatograms of the PO HDO product, showing the identified compounds along with their names and chemical formulas. . . . VI
A.3 GC-MS chromatograms of the BO feedstock, showing the identified compounds along with their names and chemical formulas. VII
A.4 GC-MS chromatograms of the BO HDO product, showing the identified compounds along with their names and chemical formulas. . . . VIII

1
Introduction

This Master's Thesis is performed in collaboration with VAROPreem. On January 16th 2026, the Swedish company Preem AB underwent a merge with VARO Energy, resulting in a brand new, leading energy company in Europe. The merge enhances the scale, production capacity and energy supply capabilities which makes it one of the world's six largest producers of renewable fuels. Before the merge, Preem was a well established energy company located in Sweden and accounting for a significant portion the transportation fuel demand all over Scandinavia. Since 2010, Preem has invested in renewable fuels with the aim of reducing the carbon footprint across the entire fuel value chain. Preem, now VAROPreem, operates two major refineries in Sweden located in Lysekil and Gothenburg with the opportunity to utilize renewable raw materials in already existing processes. This supports the ongoing transition towards more sustainable fuel production.

The efforts provided by VAROPreem are expected to increase renewable fuel production capacity by various research and upgrading refinery units to enable co-processing of renewable feedstocks. In short, VAROPreem is a strong leading force in the development and production of renewable fuels and enables the execution of this project.

1.1 Background

Climate change is one of the largest threats to our modern society facing for example global temperature rise and melting ice sheets. The current warming of the earth is occurring at a rate higher than for the past 10 000 years [4]. One of the main causes of climate change is the transportation sector as it is a major contributor to the accumulation of greenhouse gases (GHGs) in the atmosphere [5]. Road transport accounts for a large share of these emissions due to the combustion of petroleum based fossil fuels, while emissions from aviation and shipping continue to increase. Overall, the transport sector as a whole contributes to approximately one quarter of the global carbon dioxide emissions and a fifth of EU emissions [5, 6]. Therefore, the global energy system is under a major transformation driven by the need to reduce the amount of emissions. Mitigating GHG emissions from the transportation sector is essential and can be achieved through three main routes including improving vehicle efficiency, reducing transport and replacing fossil fuels [7]. The outcomes of the COP28 highlight the need to move away from fossil fuels within the coming decades

[8]. Sustainable alternatives including liquid bio-fuels offer several benefits over the conventional fuels used today. Apart from reducing emissions, bio-fuels can possibly play an important role by improving energy efficiency, improve energy security and contribute to economic development [9].

Bio-fuels are fuels derived from organic materials refereed to as biomass. Multiple different sources are included in the term biomass such as agricultural crops, forestry biomass and organic waste streams. Different bio-fuels can be classified, based on the origin of their feedstocks, into four generations. First generation bio-fuels are produced from food-based crops including corn, sugarcane and vegetable oils. Typical examples are biodiesel produced through transesterification [10] and bioethanol derived from converting sugar and starches to glucose and further fermented to form ethanol [11]. Fuels based on first generation bio-fuels are relatively developed and commonly used but their usage is debated because of the competition with food supply and land use [12]. Therefore, second generation bio-fuels are developed to be derived from non-food biomass, which removes the competition for food production and offer greater potential for reducing the emission of GHGs [12]. Several examples of biomass refereed to as second generation bio-fuels are lignocellulosic materials including agricultural residues and forestry by-products. These feedstocks serves as promising renewable alternatives with potential to be incorporated in already existing refinery infrastructure [10, 13]. This allows for continued use of current systems without requiring complete replacement. However, the conversion of these types of feedstocks are more complex in terms of requiring advanced, not yet fully developed, processes and techniques. Thus, there are still challenges finding appropriate feedstock to ensure low production cost and large scale production [14].

Today's fuel supply is mainly derived from petroleum which through fractional distillation and further refining processes result in products such as diesel and gasoline. Diesel fuel contains hydrocarbons, generally in the range of 8-21 carbons with boiling points from 200-325 °C [15] and includes a mixture of saturated and aromatic hydrocarbons. These are nonpolar and contain little to no oxygen in their molecular structure. In contrast to diesel, renewable alternatives such as bio-oils are highly oxygenated with complex chemical structures resulting in an acidic, viscous and chemically unstable mixture of compounds [16]. Generally, forestry derived bio-oils contain multiple components including water (19-30 wt%), organic compounds that are GC/MS detectable (20-30 wt%), oligomers soluble in water (28-36 wt%) and oligomers insoluble in water (15-23 wt%) [16]. Bio-oils contain aldehydes, alcohols, carboxylic acids, esters, ethers, ketones, furans and phenols as main compounds adding up to hundreds of separate compounds [17]. The combined content and properties of bio-oils limit their direct use as fuels and requires an upgrading process in order to produce products that resemble the hydrocarbons of today's fuel supply.

There are two main upgrading processes suitable for enhancing the properties of forestry derived bio-oils, catalytic cracking [18] and catalytic hydrodeoxygenation (HDO) [17]. Catalytic HDO is an effective route for stabilizing bio-oils by elimi-

nating oxygenated compounds and stated to be one of the most promising methods [17], and is therefore also the method utilized in this project. Required for this method are high temperatures, high pressures of hydrogen gas since it consumes large amounts of hydrogen. The main bio-oils hydrotreated in this study are fast pyrolysis bio-oil (FPBO) from Pyrocell AB [19] and a confidential thermochemical bio-oil obtained through VAROPreem AB. After hydrotreatment, products are examined through various analyzing techniques including gas chromatography-mass spectrometry (GC/MS), nuclear magnetic resonance (NMR), thermal gravimetric analysis (TGA) and Karl Fischer (KF) titration.

1.2 Aim

The aim of this project is to investigate the hydrotreatment of different forestry derived bio-oils for potential future application as drop-in fuel. Hydrodeoxygenation (HDO) and mild hydrotreatment are the upgrading processes used for the goal of reducing oxygenates and produce hydrocarbons similar to conventional fuel from fossil sources. To obtain general knowledge of the techniques applied during this project, a simple triglyceride fatty acid is investigated and analyzed. Furthermore, the report will give an insight to obtained product compositions after hydrotreatment of two different bio-oils. Analytical methods will answer questions regarding the molecular structure, elemental composition and relative proportions of compounds. Information from this report can be utilized when evaluating if these bio-oils can be integrated and co-processed within an existing fuel value chain in the future. This project will help understand what the hydrogen based upgrading of bio-oils does to the molecular composition and finally how it contributes to the development of renewable fuels and the transition toward a more sustainable fuel value chain.

1.3 Limitations

In order to obtain valuable results, thorough analysis and interpretation of the results is required to establish the oil product compositions. Therefore, certain limitations are applied for the project to fit in the given time frame. One limitation is the number of feedstocks which has been narrowed down to three, requiring a total of four hydrotreatments. This limitation is presented to ensure valuable results that do not come across as stressed. The main bio-oils hydrotreated in this study are pyrolysis oil (PO) and a confidential forestry derived thermochemical bio-oil (BO). Oleic acid was additionally examined as a model compound to establish a reference case for HDO chemistry.

1.4 Outline

Chapter 2 describes theories important for the project, including information about bio-oils in general and hydrotreatment techniques used for upgrading. This section also explains the analytical techniques used to examine the product compositions of the bio-oils. Furthermore, chapter 3 clearly outlines the experimental protocol starting with materials and catalyst preparation followed by the catalytic hydrotreatments and characterization methods used to analyze the bio-oil feedstocks and products. Chapter 4 presents and discusses the results and chapter 5 presents conclusions and future outlooks.

2
Theory

2.1 Bio-oils: Origin, Composition & Challenges

Bio-oils can be derived from biomass from various origins with diverse compositions and properties. Biomass is often referred to as a complex organic solid product, mainly derived from plants making it non-fossil. Different origins of the biomass result in varying physicochemical properties including moisture content, ash composition and ratios of the lignocellulosic components. Included in the term lignocellulose are the main three structural components cellulose, hemicellulose and lignin. The characteristics of the biomass determine and influence conversion performance, efficiency, product distribution and bio-oil quality [20]. Approximately 80 % of the total biomass on earth could potentially serve as feedstock for thermochemical bio fuel production technologies [21]. Biomass is considered a second generation bio-fuel since it is mainly based on terrestrial plants and does therefore not compete with the food industry as the more developed first generation bio-fuels. Moreover, this renewable energy source does not contribute to the greenhouse effect thanks to its carbon dioxide neutrality.

The two bio-oils studied in this project are from forestry derived biomass and the feedstock is lignocellulosic with unknown ratios of the structural components. Decomposition of the lignocellulosic components is essential for converting the biomass into bio-oil and can be achieved through several different techniques. The bio-oils in this project is a fast pyrolysis bio-oil and a confidential thermochemical bio-crude. The following sections will describe the main methods used for decomposition of lignocellulosic components for bio-oil production as well as the composition and properties of the produced bio-oils.

2.1.1 Production Pathways

Bio-oils can be produced through several different routes depending on the chemical composition of the biomass feedstock. Determining factors are feedstock type, moisture content and desired product properties. The content of a specific biomass impact the characteristics of the final bio-oil [22]. One of the bio-oils examined in this project is produced through fast pyrolysis hence referred to as pyrolysis oil. The second bio-oil is a confidential thermochemical bio-crude and the production pathway is unknown.

Fast pyrolysis is one thermochemical conversion process which is based on the rapid decomposition of biomass at elevated temperatures in the absence of oxygen. Prior to processing, the feedstock must be dried in order to decrease the water content of the produced bio-oil since excess water reduces thermal efficiency [23]. The conversion includes heating the biomass to a temperature of approximately 550°C with a high heating rate and a residence time of less than two seconds, followed by rapid cooling [24, 25]. In this process, pyrolysis gas, vapors and char are produced simultaneously and yields depend mainly on the biomass composition and pyrolysis temperature. Generally, higher proportions of cellulose result in a higher yield of bio-oil. Other parameters influencing the liquid bio-oil are particle size of feedstock, heating rate, flow rate of carrier gas and holding time [21]. Char is removed before the vapors are condensed to produce the desired dark brown liquid bio-oil [26]. Reaction conditions are critical, since vapors remaining at reaction temperature for too long reduce the liquid yield by secondary cracking resulting in non-condensable gases [27]. Therefore, rapid quenching of the vapor right after fast pyrolysis is essential to increase the liquid bio-oil yield. Under optimized conditions, the product consist of up to 75 % yield of fast pyrolysis bio-oil containing 35-50 % oxygen and typically 15-25 % water [28]. Another pyrolysis processes not as suitable for bio-oil production is slow pyrolysis which operates at lower temperatures with longer residence time [22]. This method produces large amounts of solid char which reduces the liquid bio-oil yield, unfavorable from a cost perspective for fuel production.

Hydrothermal liquefaction (HTL) is another method for converting biomass into bio-oil, using wet or dry feedstock. The biomass feedstock is liquefied in the presence of a solvent for example water, methanol, ethanol or acetone at a medium temperature of 250-550 °C and a high pressure of 5-25 MPa [21]. Under these conditions, hydrolysis is promoted which thermally degrades the biomass structure and converts it into a liquid bio-oil as well as char and gases [29]. Firstly, depolymerization of biomass occurs followed by decomposition, and lastly, reactive molecules are recombined to form compounds of high molecular weight. To obtain high yields of bio-oil, specific reaction conditions are applied with temperatures of 300-350 °C, pressures of 24-27 MPa and residual times of 15-25 min [30]. After heating to the final temperature, the product is cooled down to room temperature and char and gas can be separated from the bio-oil. Bio-oils produced through HTL are generally more deoxygenated and more hydrophobic than the fast pyrolysis bio-oil [13]. To obtain high quality bio-oil, high lignin content, solvents with higher density to promote hydration reactions and factors such as pressure, heating rate and residence time is critical [21]. The yield of the final liquid bio-oil is strongly dependent on the composition of the feedstock with values varying from 30-90 % while the oxygen content is reduced from approximately 40 % in the raw biomass to between 10-15 % in the product [31].

2.1.2 Chemical Composition & Physical Properties

Bio-oils are very complex chemical mixtures, containing hundreds of organic compounds across multiple chemical families with varying properties. The complexity

is a result of thermochemical or hydrolytic fragmentation of biomass containing the three major compounds, cellulose (40-45 %), hemicellulose (25-35 %) and lignin (20-30 %) [22]. Even though bio-oils vary when derived from different materials they are often homogeneous in appearance and macroscopic single phase liquids [32]. A general overview of the major compound classes present in bio-oils are presented to understand the chemical composition and what impact it has on the properties of the oil. Water is an intrinsic component of bio-oils ranging from 15-25 % [28] in pyrolysis oil while bio-oil converted by HTL generally contains a lower, still significant, amount [13]. Water reduces the heating value of the oil and promotes instability and phase separation which makes the oil difficult to handle and process consistently. The chemical composition of a bio-oil is unstable due to the presence of oxygenated compounds classified as alcohols, aldehydes, acids, ketones, anhydrosugars and phenolics [33]. The high concentration of reactive functional groups in bio-oils continue to undergo condensation, polymerization and esterification reactions during storage. Moreover, these types of reactions lead to increases in acidity, viscosity and molecular weight over time demonstrating aging and instability [34]. Catalytic upgrading is required to improve fuel properties by lowering the oxygen content of bio-oils. Catalytic hydrotreatment is one way of increasing the stability of bio-oils by applying high pressures of hydrogen gas at elevated temperatures with the purpose of producing higher quality bio-oils.

2.2 Fatty Acids

Apart from bio-oils, fatty acids are valuable molecules researched and used for biofuel production. Unlike lignocellulosic bio-oils derived from biomass, fatty acid based oils are characterized by a relatively simple and well defined chemical composition, a higher energy density with a lower oxygen content [35]. These are all properties making fatty acids suitable for catalytic upgrading and use as drop-in fuels. The most common way of producing drop-in bio-fuels from different feedstocks is to utilize oleochemical feedstocks like vegetable oils, animal fats and waste cooking oils [36], all based mainly on fatty acids for instance oleic acid. Hydrocarbon products obtained after upgrading of oleic acid are presented in Figure 2.1 and are chemically very similar to hydrocarbons found in conventional petroleum diesel [35]. In this study, the well known and thoroughly studied fatty acid oleic acid is used as a model compound to study the impact of hydrotreatment on a simple molecule. The use of a model compound with precisely known chemical structure serves as a starting point to study individual reaction pathways.

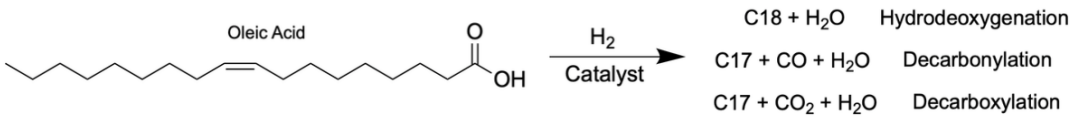

Figure 2.1: Reaction pathways for oleic acid during hydrotreatment, obtained based on information from [1].

Oleochemical feedstocks are composed primarily of triglycerides consisting of three long-chain fatty acids attached to one glycerol with a molecular structure similar to petroleum crude oil. The triglycerides differs by fatty acid chain length, their degree of unsaturation and from which type of oil [37]. One of the most abundant fatty free acid is oleic acid (C18:1) containing 18 carbon atoms and one unsaturated double bond [38]. Triglyceride based oils generally contain a lower oxygen content than bio-oils derived from forestry biomass, ranging from 8-22 % [37] concentrated in the ester linkages of the triglyceride structure and the carboxyl groups of the free fatty acids. This oxygen is comparatively straight forward to remove and separates the triglycerides through hydrotreatment, making fatty acid based feedstock attractive for catalytic upgrading.

Hydrotreated vegetable oil (HVO) is a commercially available paraffinic drop-in fuel primarily based on vegetable oil derived from food crops such as soybean, sunflower, rapeseed and palm oil [39], making it a first generation biofuel competing with food production. HVOs are straight chain paraffinic hydrocarbons, free of sulfur and aromatics [40]. The pure form of this fuel is refereed to as HVO100 and is produced by catalytic hydrotreatment where the triglycerides are first hydrolyzed to free fatty acids and glycerol, and the fatty acids are further deoxygenated to yield straight chain hydrocarbons [39]. Resulting is a product fully compatible with existing diesel engines and lowers the carbon dioxide emissions by 80-90 % [41]. Oleic acid is a key constituent of the triglyceride feedstocks used in HVO100 production.

2.3 Catalytic Hydrotreatment

Bio-oils showcase several unfavorable properties that prevent them from being directly utilized as fuels. These include high oxygen content resulting in high acidity, chemical instability that leads to polymerization, elevated viscosity and low energy density [42]. Polymerization of the bio-oil components can cause the formation of coke which is seen as the bottleneck issue for converting bio-oil into bio-fuel by conventional methods [43]. In addition, bio-oils are made up of very complex compositions and contain high water content and is highly viscous, further indicate the need for upgrading [33]. Catalytic hydrotreatment is therefore considered a key upgrading strategy used to produce hydrocarbons more suitable for fuel applications.

The main principle behind hydrotreatment is to react the liquid bio-oil with high pressure hydrogen gas at elevated temperatures to improve its chemical and physical properties [16]. The catalyst serves to lower the activation energies of the desired reaction pathways such as hydrogenation and deoxygenation, while suppressing polymerization and coking. Hydrotreatment methods can be classified based on their severity and the intended purpose of the process, as they are applied to achieve different outcomes. In short, the main objective is to reduce heteroatoms in bio-oils by

hydrogenation, deoxygenation, decarboxylation and dehydration as main reactions [3]. This increase the hydrogen to carbon ratio and reduce heteroatom content, resulting in improved energy density and thermal stability, factors that enhance the compatibility with existing fuel infrastructure.

At the molecular level, hydrotreatment involves several interconnected key reactions that progress simultaneously and competitively, depending on reaction conditions and catalyst used. Hydrogenation initially saturates the unsaturated bonds of C-C and C-O double bonds through reaction with hydrogen [2] with an example shown in Figure 2.2. Since double bonds are the main drivers for undesirable polymerization, this step is essential to suppress coke formation and high molecular weight oligomers. By saturating these groups, the liquid yield increase and the catalyst is not as easily deactivated which promotes further reaction through deoxygenation [44]. After saturating the bonds, deoxygenation reactions can proceed to remove oxygen atoms in the form of water, carbon monoxide or carbon dioxide depending on reaction conditions and reaction pathways [45]. Together, these reactions convert the properties of complex bio-oils closer to conventional fuels by stabilizing and reducing the oxygen content.

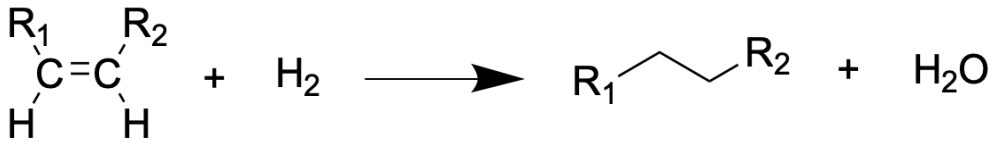

Figure 2.2: Hydrogenation reaction associated with catalytic hydrotreatment for bio-oil upgrading. Drawn on the basis of information from [2].

Hydrotreatment processes can be conducted in either batch or continuous reactor systems. Batch reactors are often applied at laboratory scale due to their operational simplicity and cost effectiveness since it allows for testing of reaction conditions and small batches [34, 46]. Continuous fixed-bed reactors are more representative in industrial applications since that can operate in steady state and allows for scalability. Lately, more efforts have been put in developing pilot plants for continuous reactors for research [47]. Also, char and coke production during reaction is continuous systems is lower compared to batch type reactors [48]. In this study, a batch reactor system is utilized for all hydrogen treating experiments.

Lastly, the hydrotreatment in this study is further classified based on reaction conditions into mild hydrotreatment and HDO. Mild hydrotreatment is conducted at lower temperatures to initially stabilize the pyrolysis oil before performing HDO, mainly to reduce the formation of char [34]. One of the most important and relevant processes for bio-oil upgrading is hydrodeoxygenation (HDO), which is discussed in

detail in the following section.

2.3.1 Hydrodeoxygenation (HDO)

Hydrodeoxygenation (HDO) is a catalytic hydrotreatment process where oxygen is removed from compounds in the presence of hydrogen. HDO can be conducted under varying degrees of severity depending on the desired outcome. Severe conditions aim for near complete deoxygenation to produce hydrocarbon fuels compatible to use as drop-in fuel in existing infrastructure. However, increasing severity also leads to higher hydrogen consumption, potential carbon loss and catalyst deactivation due to coking or poisoning. Besides producing deoxygenated products, HDO release water but also CO and CO_2 through decarbonylation and decarboxylation [3]. The removal of oxygen during HDO can occur through several reaction pathways presented in Figure 2.3. Direct HDO removes oxygen as water through C-O bond cleavage, a pathway associated with significant hydrogen consumption that may also involve saturation of unsaturated bonds. HDO reactions proceed through compound class dependent pathways, where phenolic and furanic compounds are among the most difficult to fully deoxygenate [49]. Overall, HDO reactions reduce polarity and the O/C ratio and produce compounds with properties resembling those of conventional fuels.

Figure 2.3: Hydrogenation reaction associated with catalytic hydrotreatment for bio-oil upgrading. Drawn on the basis of information from [2, 3].

In this study, HDO is applied to all investigated feedstocks as the main upgrading step. To ensure that the HDO treatment operates efficiently, the reaction conditions and choice of catalyst serves an important role. Which catalyst are applied and why, is stated in the next section focusing on the purpose of the different catalysts.

2.4 Catalysts

Catalysts are crucial components in the process towards improving bio-fuel properties and reduce coke formation during hydrotreatment. A variety of catalysts can be applied to reduce the oxygen content hence stabilizing bio-oil feedstocks. In this project, the heterogeneous catalysts Pd/C and $NiMo/Al_2O_3$ are used in hydrotreatment of bio-oils and consist of two main components. Metal particles that serve as the active site for hydrogenation reactions and a support material that stabilizes these particles, increases the surface area and provides additional basic or acidic

functional sites [16].

Noble metal catalysts are applied for mild hydrotreatment at lower temperatures with the purpose to stabilize the bio-oil by hydrogenation of reactive compounds to less active corresponding alcohols. In this stage, mainly carbonyl and carboxyl functional groups and sugars are transformed into alcohols, increasing the H/C ratio significantly while the O/C ratio remains more similar to the feedstock [50]. For this application, noble metal catalysts are highly attractive due to their high reactivity for hydrogen activation, tolerance to deactivation in high water environments and high stability [51]. Noble metal catalysts are not yet widely adopted in industrial applications since regeneration and high prices are limiting factors despite observed improvement of the H/C ratio [52].

Sulfided catalysts are applied in hydrotreatment processes to reduce the amount of oxygen by hydrogenation, deoxygenation reactions and cracking [16]. For the NiMo catalyst, nickel is used as a promoter, donating electrons to molybdenum which creates sulfur vacancies acting as active sites for HDO reactions [51]. Adding sulfur to the feed is crucial to keep the catalyst sulfided and active, however this can cause the produced bio-fuel to contain undesirable sulfur. Oxygen containing functional groups adsorb to the sulfur vacancies undergo C-O bond cleavage and the neighboring S-H groups supply the activated hydrogen needed for deoxygenation [53]. The main role of sulfided catalysts is to reduce the oxygen content, although their performance is limited by catalyst deactivation and the need for severe reaction conditions.

2.5 Analytical Methods

This section presents the principles behind the analytical techniques utilized throughout the course of this project and describes why it is relevant for this study.

2.5.1 Gas Chromatography-Mass Spectrometry

Gas chromatography-mass spectrometry (GC-MS) is a widely used analytical technique used for characterization of complex bio-oil mixtures. It combines a gas chromatograph to separate the sample compounds and a mass detector to analyze the resulting molecules [54]. Two dimensional GC-MS with flame ionization detection (GCxGC-MS/FID) enables identification of volatile and semi-volatile organic compounds and can be used to determine concentration [55]. Due to the complexity of bio-oils and the large molecular weight ranges and various functional groups, GS-MS is not sufficient to obtain comprehensive results. Since GC-MS only detects volatile and semi-volatile species, additional and complementary methods are necessary to obtain a more complete characterization of the bio-oils [56].

2.5.2 Nuclear Magnetic Resonance

Another characterization method is nuclear magnetic resonance (NMR) spectroscopy which complements GC-MS and gives a broader picture of the structural composition of the sample. Compared to the limited GC-MS characterization range, NMR has the conditions to analyze the composition of the entire bio-oil [56]. Nevertheless, the complexity of the bio-oils makes such direct structural analysis difficult to achieve. One limitation of this method is the difficulty regarding identification of individual compounds due to the presence of overlapping peaks, making this method more suitable to analyze changes in functional group composition [57]. One dimensional quantitative ^{1}H-NMR experiments mainly produce results displaying separate regions associated with different functional groups and chemical environments. Furthermore, information about specific chemical shifts, diffusion and amplitude can be obtained through NMR [56].

2.5.3 Thermogravimetric Analysis

Thermogravimetric analysis (TGA) is a common characterization method used to study the thermal degradation of small fuel samples [58]. Materials that can thermally degrade or decompose can be characterized and the composition can be determined. TGA curves are obtained and determines reactivity through measuring mass losses as a function of time and temperature [58].

2.5.4 Karl Fischer titration

An important property of a bio-oil is their water content since it impact the properties of the oil. In order to determine the water content, Karl Fischer is a standard titration technique applied for fast and accurate determination of the water content in petroleum products.

3

Methods

3.1 Materials

Feedstocks used were a pyrolysis oil based on sawdust and a confidential thermochemical bio-oil which both were provided by VAROPreem (Gothenburg, Sweden) used for upgrading through hydrotreatment. Oleic acid was used as an additional reference feedstock (Sigma-Aldrich). For catalyst preparation, the metal precursors used were Ammonium molybdate tetrahydrate, $(NH_4)_6Mo_7O_{24}{\cdot}4H_2O$ (99.98%), and Nickel(II) nitrate hexahydrate, $Ni(NO_3)_2{\cdot}6H_2O$ (99.99%) (Sigma-Aldrich). The second catalyst used in this study was a commercially available Palladium on Carbon (Pd/C) catalyst (Sigma-Aldrich). Dodecane (C12) and hexadecane (C16) were used as solvents during hydrotreatments (Sigma-Aldrich). Dimethyl disulfide (DMDS, $\geq$ 99.0%) was used as sulfiding agent for the sulfided $NiMo/Al_2O_3$ catalyst. Gases applied were high-purity Hydrogen Detector 5.0 (99.999%) and Cronigon S2 (98.0% Ar, 2.0% O_2) for hydrotreatment experiments and catalyst passivation respectively. For analysis, additional chemicals from Sigma-Aldrich were used without any modification or purification.

3.2 Catalyst Preparation

One of the catalysts used is the Nickel-Molybdenum (NiMo) catalyst which is supported on Al_2O_3. The $NiMo/Al_2O_3$ catalyst is prepared through a conventional incipient wetness co-impregnation of the support and an aqueous solution of the Ni and Mo precursors. The used precursors and are nickel(II) nitrate hexahydrate, $Ni(NO_3)_2{\cdot}6H_2O$ (2.686 g) and ammonium molybdate tetrahydrate, $NH_4)_6Mo_7O_{24}{\cdot}4H_2O$ (3.592 g). The Al_2O_3 support (11 g) was weighed and calcined at 550 °C for 8 h. On the second day, the Nickel and Molybdenum loadings are impregnated drop-wise on the support followed by drying at 60 °C for 24 h and 110 °C for 24 h. Lastly, the powder was again calcined at 550 °C for 12 h with a heating rate of 2 °C min^{-1}.

3.2.1 Catalyst Activation

To activate the catalysts before hydrotreatment, a sulfidation process is applied for the $NiMo/Al_2O_3$ catalyst and the metal catalyst Pd/C is reduced. The reaction conditions for the two different activation processes are presented in Table 3.1. After performing the activation processes, the bio-oil feed can be added to the vessel and catalytic hydrotreatment is performed.

Table 3.1: Reaction conditions for the activating processes of the catalysts used for hydrotreatments.

Experiment	Catalyst	Temperature (°C)	Hydrogen pressure at room temperature (bar)	Time (h)
Sulfidation	$NiMo/Al_2O_3$	340	20	4
Reduction	Pd/C	300	15	4

The $NiMo/Al_2O_3$ catalyst is sulfided using dimethyl disulfide (DMDS). The desired amount of catalyst (2 g) is loaded into the reactor and sulfided by 500 μl of DMDS at a pressure of 20 bar H_2 at room temperature. Furthermore, the temperature is set to 340 °C for 4 h. During the process, DMDS decomposes and reacts with hydrogen, producing the sulfiding agent H_2S. For experiments using $NiMo/Al_2O_3$ as catalyst, an additional 100 μl of DMDS is added to the feed to maintain catalyst sulfidation during the reaction. For the Pd/C catalyst, the pre-treatment involves reducing the noble metal catalyst by introducing a pressure of 30 bar H_2 at room temperature for 4 hours and at 300°C. Lastly, passivation is performed when the reduction is finished by running argon gas containing 2% oxygen gas through the system for 1 h after flushing the reactor with N_2. The flow of the introduced gas is constant and around 25-30 ml/min, controlled by an ADM Flow Meter (Agilent).

3.3 Hydrotreatment Experiments

3.3.1 Reactor Setup

All experiments, including catalyst activation and hydrotreatments are conducted in a stainless steel batch reactor autoclave (Parr Instruments, 450 ml) equipped with an impeller stirrer. A heating system (Parr 4848 reactor controller) is applied with the purpose of controlling reaction conditions. The pressure and temperature is altered depending on the experiment and the type of bio-oil. For all stabilization and HDO experiments, a stirring rate of 1000 rpm is applied from the time of setting the reaction temperature. For oleic acid, a stirring rate of 100 rpm is applied until the reaction temperature is reached, then the stirring rate is increased to match the

remaining experiments at 1000 rpm.

3.3.2 Stabilization and Hydrodeoxygenation

After loading the feedstock and assembling the reactor, the vessel is purged and depressurized three times with nitrogen (6 bar). This is followed by purging hydrogen, starting with a low pressure to perform leak testing several times at increasing pressures. Lastly, the desired pressure of H_2 at room temperature is achieved through charging hydrogen gas into the vessel until the final pressure is reached. Reaction conditions for the hydrotreatments along with catalysts, solvents and feedstock loadings used for each experiment are listed in Table 3.2. A pre-set reaction time of 4 h is applied for the entire set of experiments.

Table 3.2: Reaction conditions, catalysts and oil loadings used for hydrotreatment of the bio-oils.

Experiment	**Temp. (°C)**	**H_2 pressure at room temp. (bar)**	**Catalyst**	**Feed**	**Time (h)**
HDO Oleic Acid	325	30	1 g $NiMo/Al_2O_3$	Oleic acid (15 wt%) in dodecane, total volume 100 ml	4
Pyrolysis Oil Stabilization	250	30	1 g Pd/C	10 g PO in 100 ml hexadecane	4
HDO Stabilized Pyrolysis Oil	400	30	2 g $NiMo/Al_2O_3$	Entire hexadecane phase from PO Stabilization	4
HDO Thermochemical Bio-Oil	400	30	2 g $NiMo/Al_2O_3$	10 g BO in 100 ml hexadecane	4

For the hydrotreatment of oleic acid, a solution of 13 ml oleic acid and 87 ml of dodecane is prepared to obtain the total volume 100 ml with 15 wt% oleic acid. The feed is added to 1 g of the sulfided $NiMo/Al_2O_3$ catalyst and the temperature is set to 325 °C with a stirring rate of 1000 rpm, held for 4 h. During heating from room temperature, the stirring speed is set to 100 rpm to not promote reaction before the final temperature is reached. The reaction time of 4 hours is recorded from the time that the set temperature is reached.

For the mild hydrotreatment, a total of 10 g pyrolysis oil is added together with 100 ml of hexadecane to 1 g of the reduced Pd/C catalyst. After the mild stabilization step, 2 g of the $NiMo/Al_2O_3$ catalyst is sulfided prior to the following HDO experiment. The feed used for this is the liquid hexadecane phase obtained from the mild hydrotreatment. This second step of treatment is conducted at 400 °C with a pressure of 30 bar at room temperature for 4 h. Stirring at 1000 rpm is applied when setting the temperature. Lastly, HDO for the thermochemical bio-oil is conducted at the same reaction conditions and feed loading as HDO of the pyrolysis oil.

3.3.3 Sample Collection

Feedstocks of the different bio-oils are saved for analysis and samples from hydrotreatment are collected after each experiment. From the reactor, samples are collected in beakers before being used for analysis. After each experiment, the product in the vessel is poured onto a glass filter (size 4) which separates the solid and liquid product through filtering demonstrated in Figure 3.1. The hexadecane phase of the liquid product is separated and collected in a beaker before cleaning out the remains in the vessel with acetone which is poured through the same glass filter. This creates another liquid phase refereed to as the acetone phase, also used for analysis.

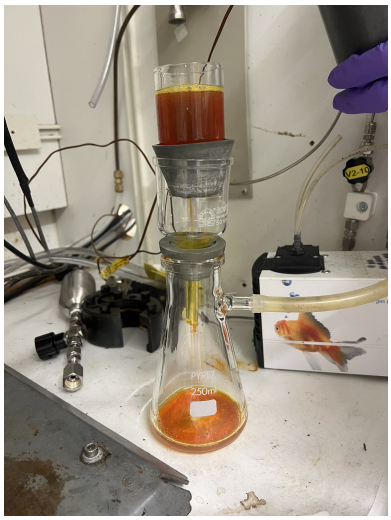

Figure 3.1: Procedure for collection of liquid samples, the glass filter collects the solid product while the liquid product proceeds through the filter.

To understand how the mass is distributed after hydrotreatment of the different bio-oils, calculations based on masses before and after treatments are conducted. Equations 3.1-3.3 showcase how solid, liquid and gas yields after the hydrotreatments are obtained,

$$\text{Yield of Solid (wt\%)} = \frac{\text{Mass of Dried Solid} - \text{Mass of Catalyst}}{\text{Mass of Feed}} \times 100\% \quad (3.1)$$

$$\text{Yield of Gas/Loss (wt\%)} = \frac{\text{Mass of Feed} - \text{Mass of Product}}{\text{Mass of Feed}} \times 100\% \quad (3.2)$$

$$\text{Yield of Liquid (wt\%)} = (100 - \text{Yield of Gas/Loss} - \text{Yield of Solid}) \times 100\% \quad (3.3)$$

where mass of feed and the mass of the products oleic acid, PO or BO is excluding the hexadecane solvent.

3.4 Product Analysis

For the two bio-oils with complex product compositions, an overall procedure is presented in Figure 3.2 which shows feedstock and product along with performed analyzing methods.

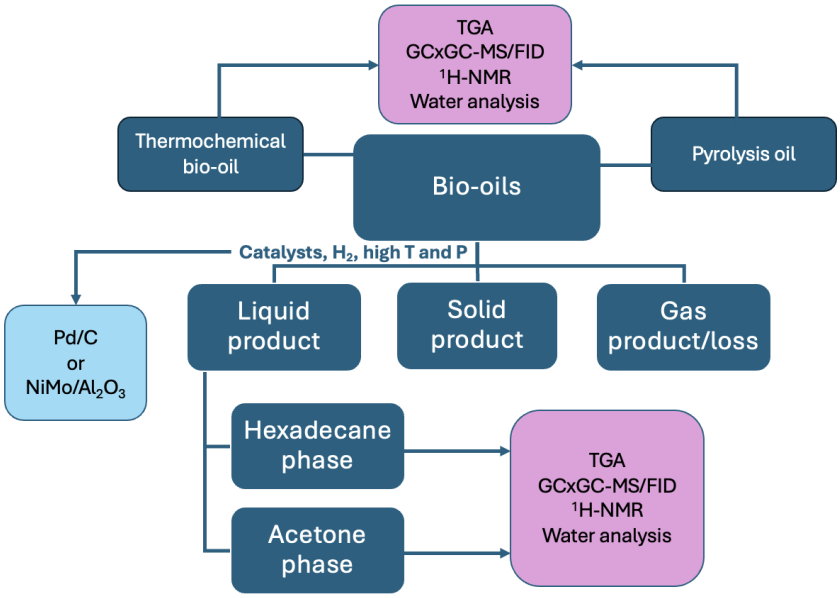

Figure 3.2: Schematic overview of the experimental workflow, including the bio-oil feedstocks, hydrotreatment process, product separation and analytical techniques used.

For the Karl Fischer analysis, the Metrohm 870 KF Titrator V20 is used to determine the water content of the samples by titrating with HYDRANAL^{TM} Composite 5 (Honeywell Fluka). Additionally, water standard (Aquastar, 1%) is used as

reference for calibration and standardized methods is applied for the hexadecane, isopropanol and acetone fractions respectively. Water content is analyzed for the feedstocks dissolved in isopropanol and after stabilization and HDO. About 0.2 mg of each sample is titrated into the solvent and all measurements are performed in triplicates with an average value reported.

To determine the boiling point distribution of the bio-oil feedstocks, thermogravimetric analysis (TGA) is performed by using the Mettler Toledo TGA/DSC 3+ Star analyzer. Approximately 10 mg of each sample is loaded into separate crucibles and heated to 600 °C from room temperature with a heating rate of 5°C min^{-1}. This procedure includes heating under an inert atmosphere with an N_2 flow of 60 Nml/min. The remaining mass in weight percentage is recorded continuously as a function of temperature creating the desired boiling point distribution for each bio-oil feedstock.

^{1}H-NMR was performed to further analyze the structural composition of the bio-oil feedstocks and liquid products obtained through hydrogen upgrading. Two different solvents are applied for the feedstocks and liquid product fractions. Deuterated chloroform ($CDCl_3$) is utilized for the hexadecane fractions while dimethyl sulfoxide (DMSO) is used for the feedstocks and acetone fractions. Data processing is performed using the software MestRenova.

Two-dimensional gas chromatography coupled with mass spectrometry and flame ionization detection (GCxGC-MS/FID) is applied to classify the large amount of compounds present in bio-oils and their hydrotreated products. Bio-oil feedstocks are diluted in different ratios of isopropanol determined by the viscosity. Identification of compounds is achieved through matching against the NIST library and using the hit with highest probability. In cases where the best hit returned a probability below 10%, the signal is identified as unknown and excluded from classification. Hits with a higher probability are grouped into chemical classes based on their dominating functional group by acids, sugars, furans, ketones&aldehydes, esters&ethers, alcohols and phenols. Compounds containing multiple oxygen functionalities are, in the case of no oxygen group being dominant, grouped into multiple oxygenates. Semi-quantification is performed on volume basis. For the HDO products, the hexadecane reaction solvent and cracking during the reaction result in chromatographic signals and are subtracted prior to analysis. Subtraction is possible by using a blank experiment from a previous study with identical reaction conditions and catalyst, performed in the same reactor using the same GC-MS instrument [59]. It should be noted that GC-MS primary detects volatile and semi-volatile compounds. Consequently, larger oligomers present in the bio-oils are not detected, meaning that the reported composition represents only the GC-detectable fraction of the sample.

4

Results & Discussion

4.1 Oleic Acid as Reference

The HDO of oleic acid over $NiMo/Al_2O_3$ at 325 °C and 30 bar H_2 was examined by GC-MS/FID resulting in the chromatograms in Figure 4.1 which show complete conversion of the oleic acid feedstock. The distinct peak at the retention time of 17 minutes corresponds to the oleic acid peak and disappears after treatment. Demonstrated by the fully converted oleic acid is the high activity of the $NiMo/Al_2O_3$ catalyst under given conditions, consistent with the well established capability of this catalyst for deoxygenation of fatty acids. Peaks at short retention times < 3 minutes and at 5.7 minutes are attributed to reagent residues from the derivatization and dodecane (C12) solvent, therefore excluded from the evaluated product composition.

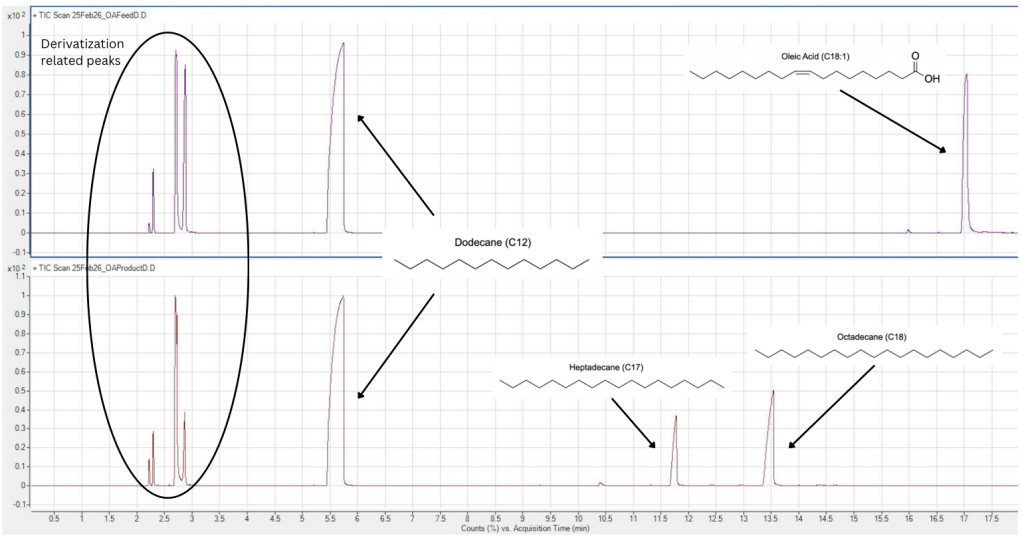

Figure 4.1: GC-MS/FID chromatogram of the oleic acid feed and product with corresponding compounds visualized.

In the liquid product, two main hydrocarbon products are identified in the GC-MS/FID chromatogram and the product is dominated by octadecane (C18) and

heptadecane (C17). The selectivity can be obtained from the peak area percentages in Table 4.1 and C18 yields 68 % while C17 account for 32 % resulting in a 2:1 ratio.

Table 4.1: Product selectivity for oleic acid HDO over $NiMo/Al_2O_3$ (325 °C, 30 bar H_2).

Compound	**Formula**	**Feed (%)**	**Product (%)**	**Selectivity (%)**
Oleic acid (C18:1)	$C_{18}H_{34}O_2$	19.71	—	—
Octadecane (C18)	$C_{18}H_{38}$	—	15.10	68
Heptadecane (C17)	$C_{17}H_{36}$	—	7.22	32
Oleic acid conversion				≥99%
C18:C17 ratio				∼2:1

Overall, these results confirm that the deoxygenation of fatty acid feedstocks under the applied conditions produce a diesel range hydrocarbon mixture dominated by C17 and C18 alkenes. Both C17 and C18 fall within the diesel boiling range available in HVO100, a commercialized, renewable fuel produced through hydrotreatment of vegetable oils [40, 39]. The aim of this section is to present the core chemistry of this process utilizing a model compound at laboratory scale. In contrast to complex bio-oils, hydrotreatment of oleic acid yield straightforward and simple results, demonstrating an ideally reactive single component substrate suitable as drop-in fuel.

4.2 Physical Properties of the Bio-oils

A visual representation of pyrolysis oil samples taken of the feedstock and after each hydrotreatment stage are shown in Figure 4.2. The PO feedstock is dark brown, characteristic of its complex oxygenated nature and contain approximately 25% water. After mild treatment the hexadecane fraction appears light yellow as in Figure 4.2a (middle vial) suggesting stabilization and hydrogenation, after HDO of the obtained fraction (right vial) the product is fully clear indicating extensive deoxygenation. The resulting light color after mild treatment is consistent with substantial reduction of furans, phenolics and their oligomers which are known to contribute to the dark color of bio-oils [34, 46, 60]. Residual color may arise from sulfur compounds and oxygen-containing species not fully converted under the mild conditions.

Furthermore, after the reaction the solids left in the reactor was washed and partly dissolved in acetone. The acetone phase obtained from the mild treatment is presented in Figure 4.2b (left vial) and exhibits a dark, almost black color. This can be due to residues present from the oil that are only soluble in the polar, water soluble acetone solvent. The products in this phase are not collected and inserted to the reactor for the HDO which in the case of containing oil residues, would affect

the results of the HDO. In short, only the fraction of oil stabilized in hexadecane after step one is used for HDO. Solely based on the transparent appearance of the acetone phase from the HDO in Figure 4.2b (right vial), no catalyst or oil residues are present.

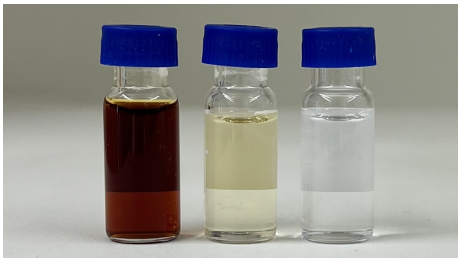

(a) From the left: PO feedstock, mild treatment product, HDO product.

(b) From the left: Acetone phase after mild treatment, acetone phase after HDO.

Figure 4.2: Physical appearance of the pyrolysis oil before, during and after the two-step hydrotreatment.

Color changes of the thermochemical bio-oil after treatment are presented in Figure 4.3 including feedstock, hexadecane phase and acetone phase. In Figure 4.3a the color of the feed is black and solved in isopropanol to become less viscous (left vial) and the pure feedstock contain approximately 10% water. The hexadecane soluble product (right vial) resulted in a dark orange color and the acetone phase in Figure 4.3b is a lighter version of the product phase, indicating a dilute version of the product with similar product composition.

(a) From left: BO feed and IPA 1:10, HDO product.

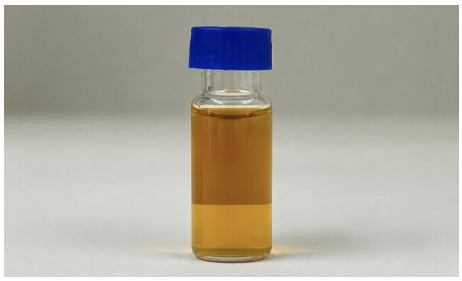

(b) Acetone phase after HDO treatment.

Figure 4.3: Physical appearance of the thermochemical bio-oil before and after HDO.

One week after hydrotreatment and storage at room temperature, both the organic hexadecane and aqueous acetone phases of the thermochemical bio-oil had become

visually darker as in Figure 4.4. This observation imply continued chemical reactions after HDO treatment, indicating an unstable product hence incomplete deoxygenation. A two step reaction similar to the one used for PO could possibly stabilize the BO and avoid aging after reaction.

(a) Immediately after treatment. **(b)** One week after treatment.

Figure 4.4: Comparison of hydrogen-treated bio-oil samples immediately after treatment and after one week of storage at room temperature. From the left: hexadecane phase, acetone phase.

4.3 Product Composition

The solid fractions of the bio-oil products are observed and the liquid compositions are analyzed and evaluated. Liquid bio-oil compositions before and after catalytic hydrotreatment are presented from ^{1}H-NMR and GCxGC-MS/FID data. The pure feedstocks are also characterized based on boiling point distribution.

4.3.1 Solid Product

Solid yields from the first step hydrotreatment of each bio-oil are presented in weight percentages relative to the 10 g bio-oil feedstock in Figure 4.5. The pyrolysis oil, reacted through an initial mild Pd/C hydrotreatment, produced a solid yield of 8.1 wt% while the following HDO step of the stabilized product produced a negligible solid fraction yielding < 1 wt%. The hexadecane fraction from the mild treatment contain stabilized product without any unstable heavy compounds and will naturally not yield solid product. Moreover, the thermochemical bio-oil directly treated through severe condition HDO over $NiMo/Al_2O_3$ produced a substantially higher solid yield of 20.8% as shown in Figure 4.5. While higher temperatures usually favors more coking, the difference also reflects compositional differences between the feedstocks rather than process severity alone. The significantly higher solid formation could be a result of the absence of a stabilizing pre-treatment for the BO, leaving reactive and heavy compounds directly exposed to HDO where condensation and polymerization can occur.

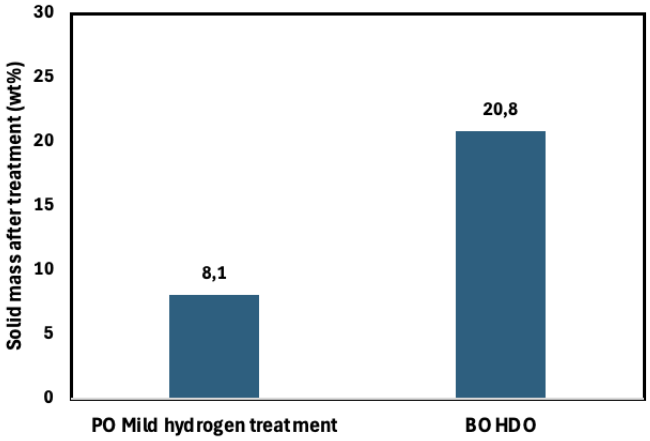

Figure 4.5: Solid product yields after the first stages of the hydrotreatments applied to PO and BO respectively.

Thermogravimetric profiles of the bio-oil feedstocks ranging from 25°C to 600°C are presented in Figure 4.6 and directly supports the higher solid yield from BO. Both curves illustrate similar shapes with an initial visual drop at approximately 100°C continuing gradually until reaching 450°C, where the mass drop start to level off. Observed is a smooth decrease in mass rather than sharp evaporation steps, supporting the claim that the bio-oils are highly complex mixtures with numerous individual compounds spanning a wide range of molecular weights and volatilities. Despite the similarities, differences in the amount of non-volatile residues remaining at 600°C are observed. At the specific reaction temperature of 400°C for HDO, PO retained 29 wt% of its mass presented in Figure 4.6a compared to 43 wt% for BO as in Figure 4.6b. This indicates a substantially higher proportion of heavy, non-volatile compounds such as high molecular weight oligomers and thermally stable oxygenated polymers which results in higher yields of solid formation during hydrotreatment.

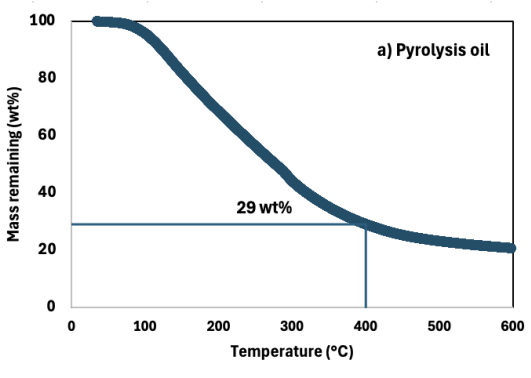

(a) TGA of PO Feedstock.

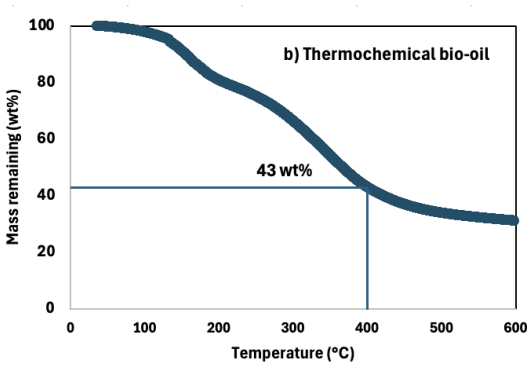

(b) TGA of BO Feedstock.

Figure 4.6: TGA of the bio-oils before hydrotreatment used to validate reaction conditions applied.

This information supports the solid yield data obtained after hydrotreatment presented in Figure 4.5, where the solid yield of the BO is higher, due to unreacted compounds incompletely converted biomass as char and carbon deposits as coke. All results presented above demonstrate the need for a stabilizing step before the harsh HDO conditions to lower the solid yield. The single step treatment at 400°C is likely to severe for the raw BO without pre-stabilization.

4.3.2 Structural Composition by NMR

The ^{1}H-NMR spectra of the hydrotreated samples are recorded in hexadecane solvent. As a consequence, the aliphatic region centered around 0.8-1.4 ppm is dominated by the strong resonances of hexadecane in all post-treatment spectra, masking product signals in that chemical shift range. Interpretation of the spectra are therefore focused on regions upfield of 2.0 ppm, where hexadecane does not contribute. Three important spectral regions containing oxygen-associated compounds are of particular relevance for monitoring the degree of HDO (i) the alpha-carbonyl/heteroatomic region (2.0-2.5 ppm), (ii) the olefinic and oxygen containing aliphatic region (2.5-5.5 ppm) and (iii) the aldehyde/aromatic region (6.5-9.5 ppm).

The ^{1}H-NMR spectra of the PO feedstock is displayed as the top spectra in Figure 4.7. In this spectra, multiple overlapping regions are observed between 3-5.5 ppm containing alcohols, esters, ethers and anomeric protons of sugar derived compounds. Additionally, multiple peaks from 1.5-2.5 ppm indicate protons present in ketones, acids and alcohols. The peaks present in the region between 6.5-7.0 ppm are from aromatic and phenolic protons mainly from furans and phenols. A distinct peak near ∼8.1 ppm is present in the feedstock, also associated with aromatic hydrocarbons probably from lignin derived oligomers. Peaks also appear around 9-0-10.0 ppm which is characteristic of aldehyde and carboxylic acid protons.

After the first mild stage of PO hydrotreatment, the ^{1}H-NMR spectrum of the product undergoes notable, specific changes compared to the feedstock visualized as the middle spectra in Figure 4.7. This step is a targeted stabilization treatment using a Pd/C catalyst rather than a deep deoxygenate step as the results indicate. At the high frequency end of the spectrum, the aldehyde peaks at ∼9.5 ppm and the aromatic carbonyl signal at ∼8.1 ppm are completely removed after the first stage of treatment. Figure 4.8 presents a representative example of carbonyl reduction of an aldehyde, corresponding to the disappearance of the ∼9.5 ppm peak. A specific observation from the spectra is the appearance of a new resonance at ∼5.8 ppm after the first stage, and probably represent intermediates formed by partial aromatic ring hydrogenation.

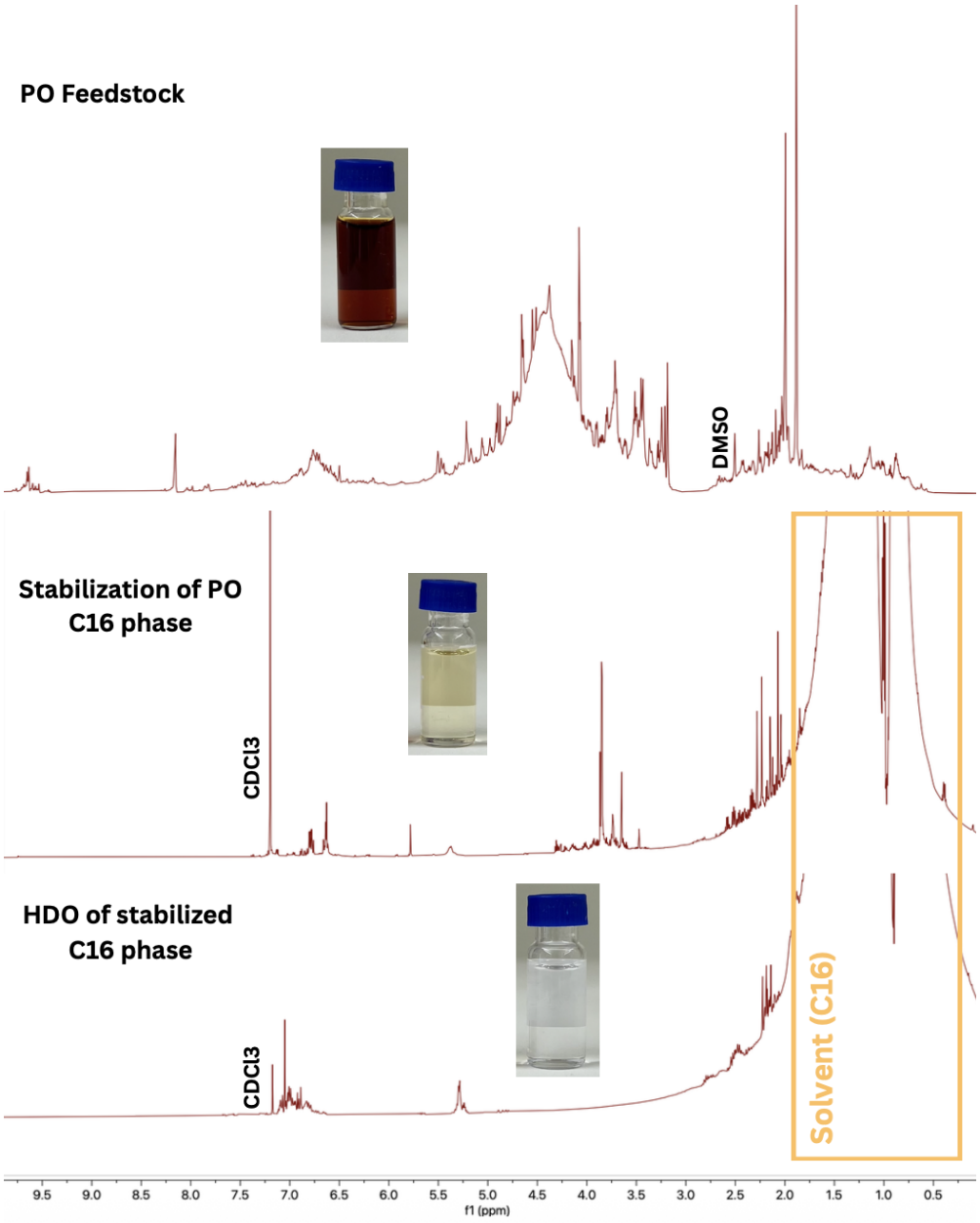

Figure 4.7: ^{1}H-NMR spectra of the pyrolysis oil, comparison between feedstock, mild stabilized product and HDO product.

Additionally, the dense region from 3.5-5.5 ppm in the feedstock is heavily reduced, but not fully removed, indicating partial reduction of methoxy groups, ethers, esters, and alcohols. More thermally and chemically stable oxygen linkages remain intact during the mild treatment. The multiple resonates between 2.0-2.5 ppm remain visually unchanged in number indicating that protons associated with ketones, acids and carbonyl species is not converted under these milder conditions. In short, the oil after stage one is selectively stabilized mainly targeting reactive unsaturated functionalities such as aldehydes, aromatics and some ether/methoxy groups.

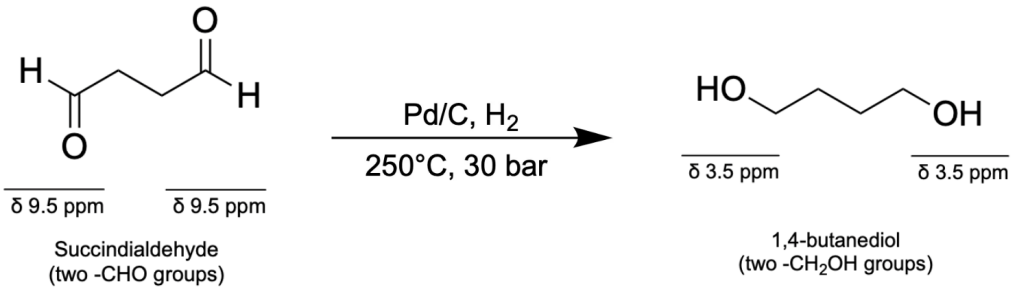

Figure 4.8: Schematic illustration of aldehyde reduction to an alcohol during mild hydrotreatment, using the conversion of succindialdehyde to 1,4-butanediol as an example.

Upon completion of the mild hydrotreatment step, the liquid product was recovered from the reactor by pouring the mobile liquid phase to yield the stabilized product inserted into the HDO. However, a residual fraction adhering to the insides of the vessel was separately recovered by rinsing with acetone. The fraction washed with acetone resulted in a dark, almost black color differing from the light pale color of the stabilized product and the differences are shown in Figure 4.9. The pronounced color difference highlights the importance to examine this fraction to provide insight into compounds excluded from the HDO experiment. The acetone solvent itself results in a singlet at 2.17 ppm in the ^{1}H-NMR spectra and overlaps with products from the bio-oil and is important to take account for when analyzing compounds in the 2-2.5 ppm region of the spectra.

Several differences are recorded, most notable is that signals reappear in the 3-3.5 ppm region of the acetone spectra, which are completely absent in the stabilized mild spectra but clearly present in the PO feedstock. Compounds contributing to these peaks, likely O-methyl groups on aromatic rings or methylene protons close to oxygen functional groups, are not converted during mild treatment with the Pd/C catalyst but deposited on the reactor walls. Thus, this indicates physical separation or deposition of these compounds rather than desired chemical removal. Furthermore, a distinct peak at $\sim$8.6 ppm consistent with aromatic systems appears only in the acetone phase and the PO feedstock, confirming that the corresponding compound class remain unreacted after the mild hydrotreatment and is not soluble in the non-polar hexadecane phase.

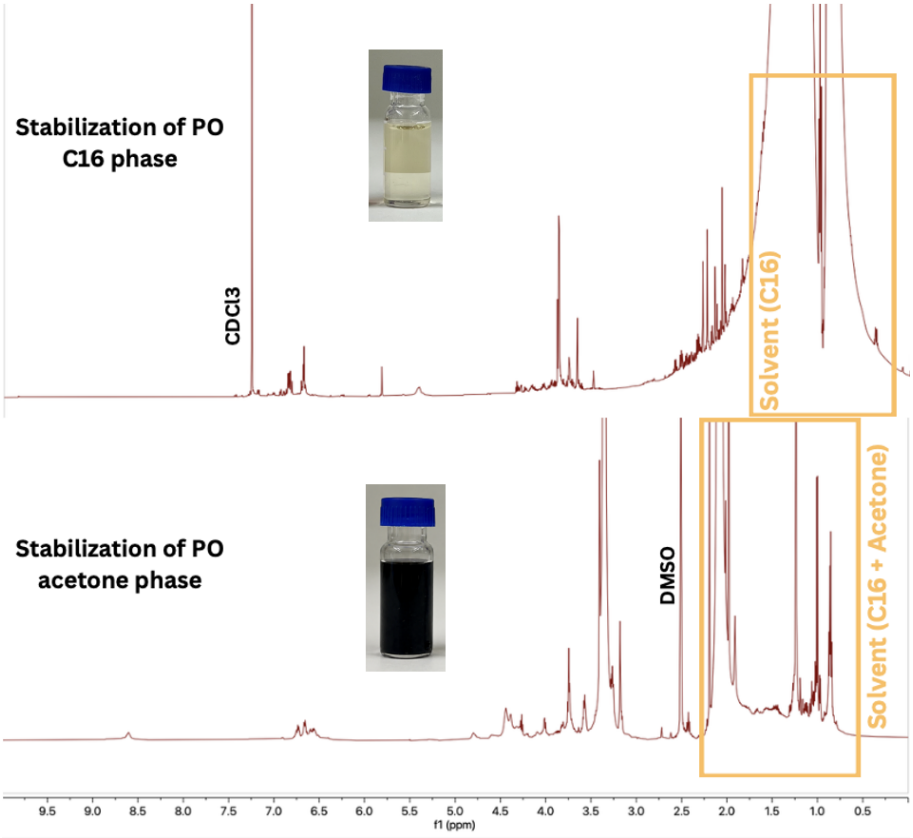

Figure 4.9: ^{1}H-NMR spectra of the pyrolysis oil, comparison between stabilized hexadecane phase and acetone fraction.

Lastly, HDO of the stabilized product at the bottom of Figure 4.7 reflects successful deoxygenation and formation of new hydrocarbon products. The most important difference after HDO treatment is the complete disappearance of all signals in the 3.5-4.5 ppm region confirming full elimination of oxygen signal that persisted through the mild treatment. Within the 2.0-3.0 ppm range, resonances between 2.125-2.5 ppm are removed and corresponds to protons from ketones and acids while remaining signals in this region could already be attributed to non-oxygenated species. New signals appearing at 7.0-7.1 ppm confirm formation of alkylated aromatic hydrocarbons while the 6.5-7.0 ppm region reflects aromatic species ranging from partially deoxygenated phenolics to fully deoxygenated alkylbenzenes. The olefinic signal at 5.4-5.5 is present during all three stages, indicating that these compounds are not reactive across both hydrogen treating stages. In contrast, the partially hydrogenated ring intermediate at ∼5.8 ppm is successfully removed after HDO.

Overall, the spectrum of the pure feedstock is highly complex, dominated by oxygenated aromatics and hydrocarbon-derived species with high oxygen functionality. This is a typical behavior of fast pyrolysis bio-oil from lignocellulosic biomass. The

mild Pd/C hydrotreatment still contain significant amounts of oxygenated aromatics and alcohols. These signals are extensively removed after the HDO treatment and one example of a two stage route for removal of oxygenates is presented in Figure 4.10. Furthermore, the key observation after HDO is the substantial deoxygenation but also ring saturation. Loss of methoxy and ether signals are extensively contributing to the desired deoxygenation while ring saturation is converting the PO toward a acyclic aliphatic hydrocarbon product more suitable for use as drop-in fuel.

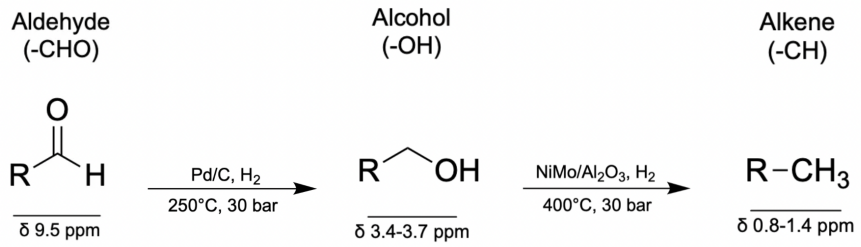

Figure 4.10: Schematic illustration of aldehyde hydrogenation to alcohol and subsequent hydrodeoxygenation to alkane.

The ^{1}H NMR spectra of the thermochemical bio-oil feedstock dissolved in IPA (1:10) and the product obtained after HDO treatment with a large fraction of hexadecane is presented in Figure 4.11. Observed is a color change that alone indicate chemical transformation during HDO. Between 6.5-7.5 ppm, a broad peak is present representing phenolic and aromatic rings from the thermochemical conversion process. Signals in the range from 2.0-3.5 ppm are consistent with ketones, carbonyl groups and aliphatic protons to aromatic rings. Small signals at 8.0-10.0 ppm correspond mainly to aldehyde and carboxylic acid protons. The overall spectral profile is difficult to interpret due to dominant solvent peaks below 2 ppm and between 3.5-5.5 ppm. However, the feedstock appears to be highly oxygenated, chemically diverse with a need for upgrading before being used for fuel production.

After single step HDO of the BO, the product is examined together with hexadecane and its fractions due to cracking. The solvent appears in the lower regions of the spectra below 2 ppm where additional hydrocarbon products mainly appear. At high chemical shifts around 8.0-10.0 ppm, all peaks disappear indicating deoxygenation of aldehydes and acids. Residual aromatic signals at 6.8-7.2 ppm remain visible which suggest aromatic rings not fully saturated under applied conditions. Moreover, peaks are observed similar to the feedstock in the range 2.0-3.0 ppm which point to oxygenated compounds such as ketones, alcohols or unsaturated carbon-carbon bonds. The distinct peak at 5.3 ppm indicates olefinic peaks or oxygen residues.

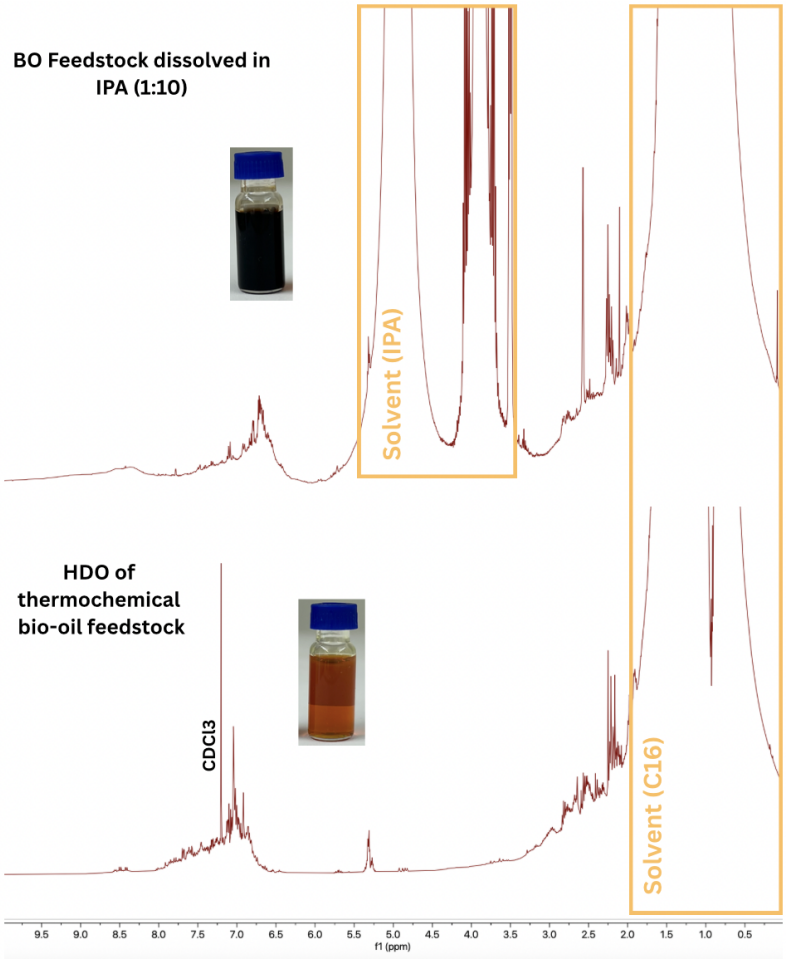

Figure 4.11: ^{1}H-NMR spectra of the thermochemical bio-oil, comparison between feedstock dissolved in IPA and HDO product.

This single step HDO of BO resulting in the two ^{1}H-NMR spectra presents data which demonstrates a product substantially more compatible with fuel streams due to the reduced amount of oxygenates. Although, the processing and conditions need further investigation to promote deoxygenation since the spectra after HDO still contain oxygenates, aromatic and olefinic content.

4.3.3 Molecular Composition by GC-MS

GCxGC-MS/FID analysis of the bio-oil feedstocks was performed to identify GC-MS detectable volatile and semi-volatile compounds which revealed complex mixtures of different components visualized in Figure 4.12. Classifications, compound names and chemical formulas of all identified compounds from the GC-MS chromatograms are presented in Appendix A. To the left in Figure 4.12a, it can be observed that the most common identified classes are multiple oxygenates (15.6 vol%), phenols (14.4 vol%) and sugars (12.8 vol%) reflecting mainly lignin- and cellulose-derived species. Accounting for around 10 vol% each are alcohols, esters&ethers and acids. Furans

and ketones&aldehydes represent smaller fractions together with non-oxygenated compounds. The remaining signal of approximately 16.5 vol% are compounds with a lower hit probability than 10 % when searching for matches in the NIST library. These findings are supported by past literature where pyrolysis oil is found to mainly consist of phenols, sugars and acids [61].

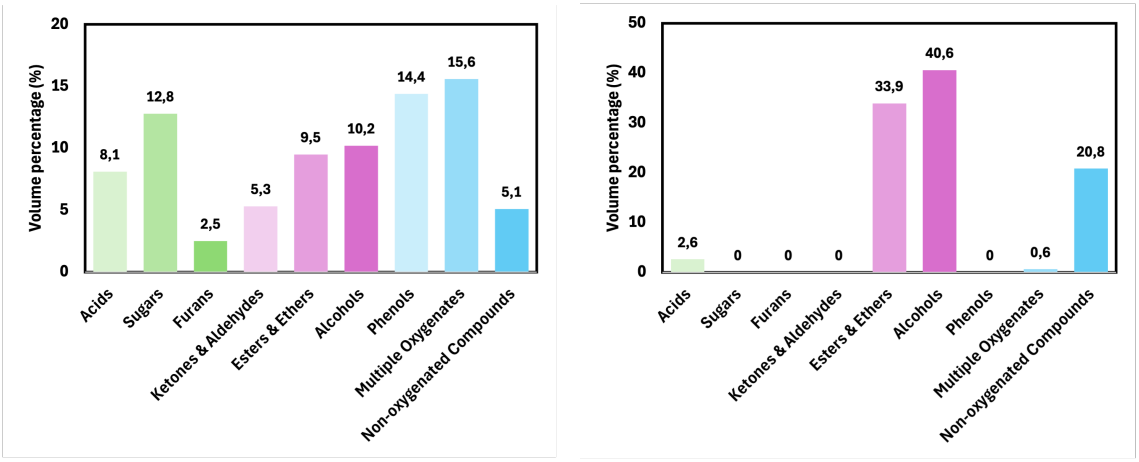

(a) Compounds in PO feedstock.

(b) Compounds in BO feedstock.

Figure 4.12: GCxGC-MS/FID data showing distribution of component classes present in the two bio-oils with classification based on identified compounds, and species with a library hit probability below 10% excluded.

In contrast to the PO feedstock where over 100 compounds are identified, the analysis of the BO feedstock only identified 17 different compounds in the GC-MS spectra, presented in Appendix A.3, due to a combination of factors rather than a single cause. Firstly, a higher dilution was applied to this feedstock due to higher viscosity which might reduce or remove the signal entirely from the spectra. Secondly, all compounds might not be soluble in the chosen isopropanol solvent. Thirdly, and more likely, is that the BO feedstock contain heavy oligomers and polymers that are not detectable in the volatility window accessible to GC-MS analysis. This is supported by previously presented residues at 600 °C from TGA data in Figure 4.6 and the solid yield of 20.8 % obtained from Figure 4.5. Out of the 17 detectable compounds, alcohols (40.6 vol%), esters&ethers (33.9 %), non-oxygenated compounds (20.8 %) and small contributions from acids and multiple oxygenates are identified as presented in Figure 4.12b. Notable is the large amount of non-oxygenated compounds, but since the few detectable components are not representative of the entire sample, no specific conclusion can be drawn from this. Absent from the detectable fraction are compounds classified as sugars, furans, ketones&aldehydes and phenols. This narrow profile represents only IPA soluble, volatile and low molecular weight compounds and does not visualize the true chemical complexity of the BO.

During HDO, the product distributions changed towards more deoxygenated products containing a majority of hydrocarbons. A classification based on functional groups and chemical structure is conducted with main focus on the hydrocarbon to oxygenate ratio. The organic, hexadecane rich, phases are evaluated by GC-MS after the final HDO experiment at 400°C and 30 bar H_2 for each oil. The compound distribution obtained after HDO of the pyrolysis oil is found in Figure 4.13 and presents a hydrocarbon to oxygenate ratio of 52,8 vol% to 35,1 vol% where the majority of hydrocarbons are acyclic aliphatic. Regarding oxygen containing components, almost only compounds under the classification ketones & aldehydes are present with minor contributions from furans, esters & ethers, alcohols and multiple oxygenates. The dominance of acyclic aliphatic hydrocarbons is consistent with ring opening during HDO, and the complete elimination of acids, phenols and sugars confirm the effectiveness of the two step treatment. Residual ketones & aldehydes open up for further optimization of the HDO process for pyrolysis oil upgrade.

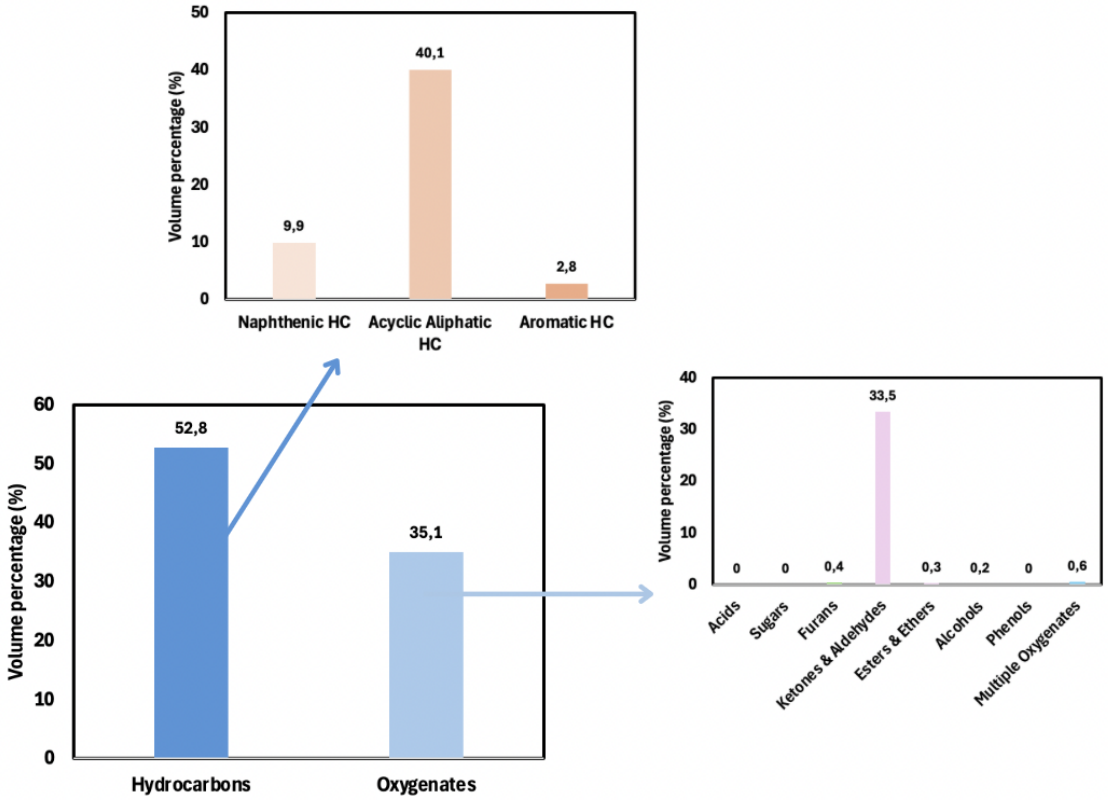

Figure 4.13: GCxGC-MS/FID product composition after hydrotreatment of the pyrolysis oil, showing the distribution of hydrocarbon and oxygenate compound classes as volume percentage, and species with a library hit probability below 10% are excluded.

After HDO of the thermochemical bio-oil, 46,4 vol% hydrocarbons and 35,1 vol% of oxygenates are identified as seen in 4.14. In this case, the distribution of naphthenic, acyclic aliphatic and aromatic hydrocarbons are more diverse and the oxy-

gen containing fraction is also more varied between functionalities. Again, the class including ketones & aldehydes is dominating but significant fractions of multiple oxygenates, esters & ethers, alcohols, acids and phenols are present. However, the persistence of these oxygenate classes indicate incomplete deoxygenation and need for other conditions or a pre-treating stabilization step as for the pyrolysis oil. Notable is that the BO after HDO includes more GC-MS detectable compounds in comparison to the pure feedstock as seen in Appendix A, indicating cracking of oligomers to lower molecular weight compounds more suitable for fuel applications.

A comparison between the two HDO products reveal differences in the obtained hydrocarbon and oxygenate fraction and the amount of undetected compounds. The PO product contained a higher hydrocarbon content (52.8 vol%) compared to the BO product (46.4 vol%), suggesting a more complete deoxygenation despite containing similar oxygenate fractions of 35.1 vol%. Even though the deoxygenation performance seem equivalent, an important factor is the amount of unidentified compounds with a low hit probability which is larger in the chromatogram for the BO.

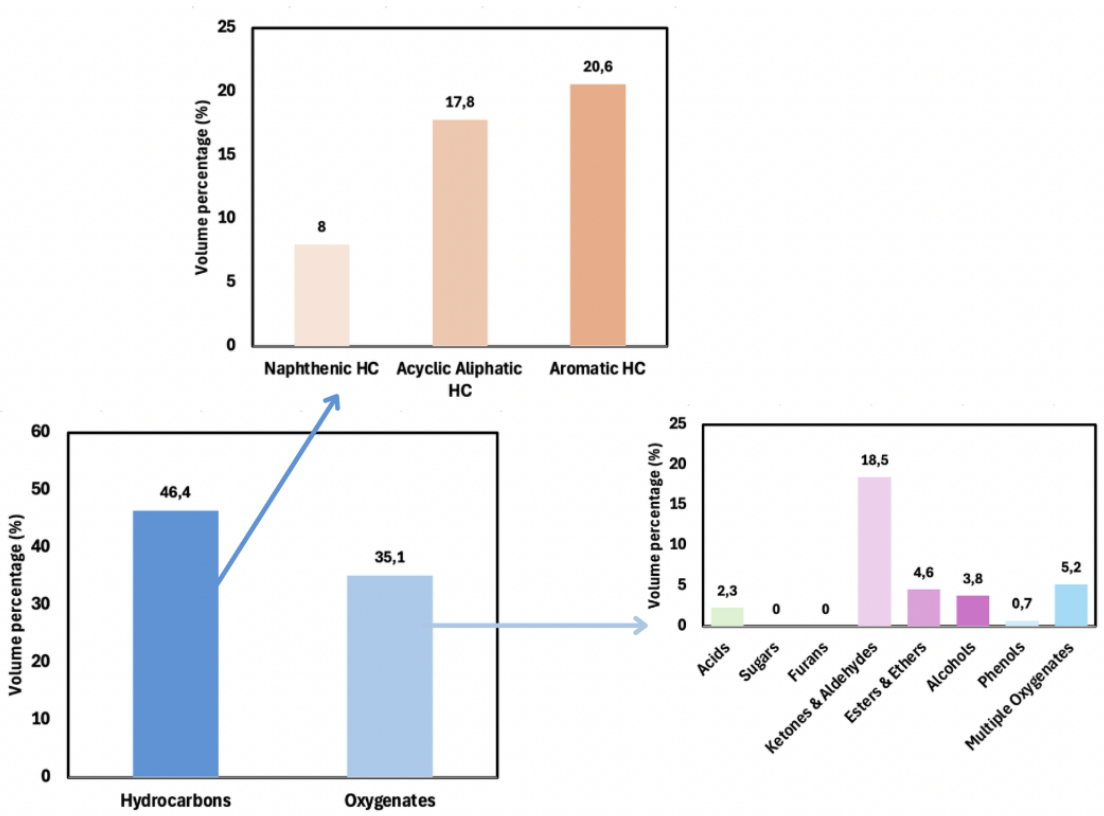

Figure 4.14: GCxGC-MS/FID product composition after hydrotreatment of BO, showing the distribution of hydrocarbon and oxygenate compound classes as volume percentage, and species with a library hit probability below 10% are excluded.

One significant compositional difference is confirmed when examining the separate hydrocarbon classification. The PO product is dominated by aliphatic hydrocarbons with only minor aromatics while the BO product contains an equal distribution between these classes. In fact, this difference could be due to both feedstock composition and processing conditions. The BO may contain more aromatic rings by nature, but the mild pretreatment to stabilize the PO could contribute to a lower aromatic content. From a fuel perspective, a higher proportion of saturated aliphatic chains are to prefer since it contributes to a higher cetane number upon combustion. Furthermore, when breaking down the oxygenate fraction to separate classes, it can be observed that ketones & aldehydes are present as main oxygenates in both HDO products. More reactive oxygenate classes are eliminated in the PO sample while various oxygenates are still present in the BO after upgrading. In short, the two step upgrading of PO produce more paraffinic, lower oxygenate product than the BO which highlight the need for optimized reaction conditions and processes for each feedstock to achieve possible bio-oil refinery integration.

5

Conclusion & Future Outlooks

Bio-oils are a promising alternative of strong interest when it comes to co-processing of renewable feedstocks for use as drop-in fuel. However, bio-oils are highly acidic, polar and chemically unstable with a low heating value, a direct consequence of their high oxygen content which present challenges for direct refinery integration. In order to achieve fuel grade properties from bio-oils, improvements are obtained through upgrading creating more stable products similar to today's fuel supply. Hydrotreatment in the form of catalytic HDO is one of the most promising upgrading strategies to address these limitations, converting oxygenated bio-oil feedstocks toward hydrocarbon rich products. The increased similarity to today's fuel enhance the compatibility with existing refinery infrastructure and engine technology.

This study evaluated the product compositions before and after catalytic hydrotreatment of two bio-oil feedstocks, pyrolysis oil (PO) and a forestry derived thermochemical bio-oil (BO). Moreover, the model compound oleic acid (OA) was used to establish a reference case for simple, fatty acid HDO reactions. The scope of this project is to characterize product compositions and classify compounds to provide clear results and significant conclusions.

Complete conversion of oleic acid was achieved at 325°C and 30 bar H_2 at room temperature over the $NiMo/Al_2O_3$ catalyst. The product consist of 60% octadecane (C18) and 29% heptadecane (C17) giving a HDO:DCO ratio of 2:1 directing the deoxygenation towards the desired HDO pathway. This process recreates the core chemistry utilized in industrial production of HVO100, at laboratory scale. The hydrocarbon product is miscible with dodecane (C12) which further confirms its suitability as renewable feedstock for refinery co-processing.

The widely studied pyrolysis oil underwent two-step upgrading, starting with a mild hydrotreatment over Pd/C at 250°C followed by HDO over $NiMo/Al_2O_3$ at 400°C. This route demonstrated advantages over single step treatment for the thermochemical bio-oil. One example is the lower yield of solid from the mild treatment

(8.1%) compared to the direct HDO of the BO (20.8%), showing the benefit of a pre-stabilizing step of reaction in suppressing coking and polymerization. The pyrolysis oil went from a dark brown, vicious liquid to a transparent, low viscosity liquid. ^{1}H-NMR analysis of PO confirmed an increased H/C ratio and removal of the most carbonyl and carboxyl functional groups, resulting in a stabilized product more suitable for HDO. During HDO, further deoxygenation of additional oxygen functionalities such as alcohols are removed. Moreover, GCxGC-MS/FID of the PO feedstock showed a highly oxygenated environment with over 100 identified compounds mainly from the classes sugars, phenols and multiple oxygenates. The final HDO product confirmed a composition dominated by hydrocarbons (52.8%) mainly consisting of acyclic aliphatic hydrocarbons. The oxygenate fraction is reduced to aldehydes & ketones while sugars, acids, furans and phenols are fully eliminated.

The thermochemical bio-oil represents a novel feedstock in the context of hydrotreatment and the first reported HDO is conducted in this project. Process and condition optimization is important to evolve and find suitable approaches for specific bio-oils. This requires years to achieve and takes much more time and research than this project allows. As a first step towards understanding how this oil behaves at harsh reaction conditions over $NiMo/Al_2O_3$, a one-step HDO approach was applied. Relative to the two-step PO result, the solid yield of this bio-oil after reaction is substantially higher demonstrating the importance of stabilization before HDO in suppressing formation of coke and char. ^{1}H-NMR analysis showed, despite disturbance of solvent peaks, elimination of aldehydes and absence of alcohol, ether and phenolic related peaks in the HDO product. The molecular composition examined through GCxGC-MS/FID presented a product distribution of only 17 components in the feedstock, pointing towards polymerized and heavy oligomers not detectable by GC-MS. The compositional analysis of compound distributions and component classes represent only the two dimensional GC-MS detectable portion of the sample. Therefore, the undetected fraction of the BO remains unknown and may contribute significantly to the overall bio-oil composition. After HDO treatment, a greater number of compounds could be identified and 46.4% corresponds to hydrocarbons where the distribution between aromatic and aliphatic are relatively similar. In comparison to the two-step PO treatment, the hydrocarbon percentage and amount of acyclic aliphatic is greater. Also, the remaining oxygenates are distributed among many different functionalities, indicating partial deoxygenation. Again, these facts are all pointing towards that the two-step hydrotreatment with a stabilizing step prior to HDO is more favorable for bio-fuel production.

The results of this study encourage multiple concrete examples for future work in this field and on these specific feedstocks. Firstly, and most notable is the application of the two-step hydrotreatment to the thermochemical bio-oil where stabilization is conducted at 250°C followed by HDO at 400°C. This is to evaluate if the pre-stabilization results in a lower solid yield and a higher acyclic aliphatic hydrocarbon percentage after HDO. Furthermore, temperature optimization for different

feedstocks and hydrogen treating steps are essential to obtain desirable products from a fuel production point of view. Characterization of the solid fractions would give information of wether it is unreacted oil or coke formation. Further analytical methods applied to both feedstocks and products including total acid number (TAN), average molecular weight by gel permeation chromatography (GPC) and elemental composition for determination of the higher heating value (HHV). This type of information would give a more comprehensive overview of the bio-fuel properties beyond product composition alone.

Bibliography

[1] Boonyawan Yoosuk, Paphawee Sanggam, Sakdipat Wiengket, and Pattarapan Prasassarakich. Hydrodeoxygenation of oleic acid and palmitic acid to hydrocarbon-like biofuel over unsupported ni-mo and co-mo sulfide catalysts. *Renewable Energy*, 139:1391–1399, 8 2019.

[2] P. M. Mortensen, J. D. Grunwaldt, P. A. Jensen, K. G. Knudsen, and A. D. Jensen. A review of catalytic upgrading of bio-oil to engine fuels, 11 2011.

[3] Chengwang Zhao, Chen Hong, Jiashuo Hu, Yi Xing, Wei Ling, Bo Zhang, Yijie Wang, and Lihui Feng. Upgrading technologies and catalytic mechanisms for heteroatomic compounds from bio-oil – a review, 2 2023.

[4] National Aeronautics and Space Administration. Evidence of climate change. `https://science.nasa.gov/climate-change/evidence/`, n.d. Accessed: 2026-05-02.

[5] United Nations. Causes and effects of climate change. `https://www.un.org/en/climatechange/science/causes-effects-climate-change`, n.d. Accessed: 2026-05-02.

[6] European Parliament. Co2 emissions from cars: Facts and figures (infographics). `https://www.europarl.europa.eu/topics/en/article/20190313STO31218/co2-emissions-from-cars-facts-and-figures-infographics`, n.d. Accessed: 2026-05-02.

[7] United States Environmental Protection Agency. Routes to lower greenhouse gas emissions from transportation. `https://www.epa.gov/greenvehicles/routes-lower-greenhouse-gas-emissions-transportation-future`, n.d. Accessed: 2026-05-02.

[8] United Nations Framework Convention on Climate Change (UNFCCC). Outcome of the first global stocktake at cop28. `https://unfccc.int`, 2023. Ac-

cessed: 2026-04-17.

[9] International Energy Agency. Delivering sustainable fuels. `https://iea.blob.core.windows.net/assets/77a8c816-dc61-4668-b501-b1793a3ab2c7/DeliveringSustainableFuels.pdf`, 2023. Accessed: 2026-05-02.

[10] A. E. Atabani, A. S. Silitonga, Irfan Anjum Badruddin, T. M.I. Mahlia, H. H. Masjuki, and S. Mekhilef. A comprehensive review on biodiesel as an alternative energy resource and its characteristics, 5 2012.

[11] Abeer Kazmi, Tahira Sultana, Amir Ali, Aneela Nijabat, Gaojie Li, and Hongwei Hou. Innovations in bioethanol production: A comprehensive review of feedstock generations and technology advances, 1 2025.

[12] M. M.K. Bhuiya, M. G. Rasul, M. M.K. Khan, N. Ashwath, A. K. Azad, and M. A. Hazrat. Second generation biodiesel: Potential alternative to-edible oil-derived biodiesel. In *Energy Procedia*, volume 61, pages 1969–1972. Elsevier Ltd, 2014.

[13] Christian Lindfors, Douglas C. Elliott, Wolter Prins, Anja Oasmaa, and Juha Lehtonen. Co-processing of biocrudes in oil refineries. *Energy and Fuels*, 37:799–804, 1 2023.

[14] A. S. Silitonga, H. H. Masjuki, T. M.I. Mahlia, H. C. Ong, W. T. Chong, and M. H. Boosroh. Overview properties of biodiesel diesel blends from edible and non-edible feedstock, 2013.

[15] Chris Collins. *Implementing Phytoremediation of Petroleum Hydrocarbons*, volume 23, pages 99–108. 01 2007.

[16] Yinglei Han, Mortaza Gholizadeh, Chi Cong Tran, S. Kaliaguine, Chun Zhu Li, Mariefel Olarte, and Manuel Garcia-Perez. Hydrotreatment of pyrolysis bio-oil: A review, 12 2019.

[17] Yanfan Yang, Xuan Xu, Haodong He, Dan Huo, Xiaoyun Li, Lin Dai, and Chuanling Si. The catalytic hydrodeoxygenation of bio-oil for upgradation from lignocellulosic biomass, 7 2023.

[18] Huiyan Zhang, Chenjun Yang, Yujie Tao, Min Chen, and Rui Xiao. Catalytic cracking of model compounds of bio-oil: Characteristics and mechanism research on guaiacol and acetic acid. *Fuel Processing Technology*, 238, 12 2022.

[19] Pyrocell. Pyrocell, 2026. Accessed: 2026-06-30.

[20] M. R. Wu, D. L. Schott, and G. Lodewijks. Physical properties of solid biomass. *Biomass and Bioenergy*, 35:2093–2105, 5 2011.

[21] R. Kumar and V. Strezov. Thermochemical production of bio-oil: A review of downstream processing technologies for bio-oil upgrading, production of hydrogen and high value-added products, 1 2021.

[22] Yogalakshmi K N, Poornima Devi T, Sivashanmugam P, Kavitha S, Yukesh Kannah R, Sunita Varjani, S. AdishKumar, Gopalakrishnan Kumar, and Rajesh Banu J. Lignocellulosic biomass-based pyrolysis: A comprehensive review. *Chemosphere*, 286, 1 2022.

[23] Anthony V. Bridgwater. Review of fast pyrolysis of biomass and product upgrading. *Biomass and Bioenergy*, 38:68–94, 2012.

[24] Dinesh Mohan, Charles U. Pittman, and Philip H. Steele. Pyrolysis of wood/biomass for bio-oil: A critical review, 5 2006.

[25] Dayane M. Coutinho, Daniela França, Gabriela Vanini, Alexandre O. Gomes, and Débora A. Azevedo. Understanding the molecular composition of petroleum and its distillation cuts. *Fuel*, 311, 3 2022.

[26] Niklas Bergvall, Roger Molinder, Ann Christine Johansson, and Linda Sandström. Continuous slurry hydrocracking of biobased fast pyrolysis oil. *Energy and Fuels*, 35:2303–2312, 2 2021.

[27] Elahe Parvari, Devinder Mahajan, and Elizabeth L. Hewitt. A review of biomass pyrolysis for production of fuels: Chemistry, processing, and techno-economic analysis, 9 2025.

[28] Niklas Bergvall, Ole Reinsdorf, Olov G.W. Öhrman, and Linda Sandström. Pretreatment of fast pyrolysis bio-oil by slurry hydroprocessing. *Fuel Processing Technology*, 281, 3 2026.

[29] Ankit Mathanker, Snehlata Das, Deepak Pudasainee, Monir Khan, Amit Kumar, and Rajender Gupta. A review of hydrothermal liquefaction of biomass for biofuels production with a special focus on the effect of process parameters, co-solvents and extraction solvents, 8 2021.

[30] Hossein Shahbeik, Hamed Kazemi Shariat Panahi, Mona Dehhaghi, Gilles J. Guillemin, Alireza Fallahi, Homa Hosseinzadeh-Bandbafha, Hamid Amiri, Mohammad Rehan, Deepak Raikwar, Hannes Latine, Bruno Pandalone, Benyamin Khoshnevisan, Christian Sonne, Luigi Vaccaro, Abdul Sattar Nizami, Vijai Kumar Gupta, Su Shiung Lam, Junting Pan, Rafael Luque, Bert Sels, Wanxi

Peng, Meisam Tabatabaei, and Mortaza Aghbashlo. Biomass to biofuels using hydrothermal liquefaction: A comprehensive review, 1 2024.

[31] Shimin Kang, Xianglan Li, Juan Fan, and Jie Chang. Hydrothermal conversion of lignin: A review, 2013.

[32] Qiang Lu, Wen Zhi Li, and Xi Feng Zhu. Overview of fuel properties of biomass fast pyrolysis oils. *Energy Conversion and Management*, 50:1376–1383, 5 2009.

[33] Shoujie Ren and X. Philip Ye. Stability of crude bio-oil and its water-extracted fractions. *Journal of Analytical and Applied Pyrolysis*, 132:151–162, 6 2018.

[34] Elham Nejadmoghadam, Abdenour Achour, Olov Öhrman, Muhammad Abdus Salam, Derek Creaser, and Louise Olsson. Stabilization of fresh and aged simulated pyrolysis oil through mild hydrotreatment using noble metal catalysts. *Energy Conversion and Management*, 313, 8 2024.

[35] Paul Santner, Santiago Nahuel Chanquia, Noémi Petrovai, Frederik Vig Benfeldt, Selin Kara, and Bekir Engin Eser. Biocatalytic conversion of fatty acids into drop-in biofuels: Towards sustainable energy sources. *EFB Bioeconomy Journal*, 3:100049, 11 2023.

[36] Junming Xu, Jianchun Jiang, and Jiaping Zhao. Thermochemical conversion of triglycerides for production of drop-in liquid fuels, 5 2016.

[37] Saima Khan, Andrew Ng Kay Lup, Khan Muhammad Qureshi, Faisal Abnisa, Wan Mohd Ashri Wan Daud, and Muhamad Fazly Abdul Patah. A review on deoxygenation of triglycerides for jet fuel range hydrocarbons, 6 2019.

[38] Pantea Moradi, Majid Saidi, and Ali Taheri Najafabadi. Biodiesel production via esterification of oleic acid as a representative of free fatty acid using electrolysis technique as a novel approach: Non-catalytic and catalytic conversion. *Process Safety and Environmental Protection*, 147:684–692, 3 2021.

[39] Diogo Melo Gomes, Rui Costa Neto, Patrícia Baptista, Cristiano Pereira Ramos, Cristina Borges Correia, and Rosário Rocha. A review of advanced techniques in hydrotreated vegetable oils production and life cycle analysis, 3 2025.

[40] Hannu Aatola, Martti Larmi, Teemu Sarjovaara, and Seppo Mikkonen. Hydrotreated vegetable oil (hvo) as a renewable diesel fuel: Trade-off between nox, particulate emission, and fuel consumption of a heavy duty engine. *SAE International Journal of Engines*, 1(1):1251–1262, 2009.

[41] VARO Energy. Varo renewable diesel, n.d. Accessed: 2026-05-19.

[42] Mai Attia, Sherif Farag, and Jamal Chaouki. Upgrading of oils from biomass and waste: Catalytic hydrodeoxygenation, 12 2020.

[43] Xun Hu, Zhanming Zhang, Mortaza Gholizadeh, Shu Zhang, Chun Ho Lam, Zhe Xiong, and Yi Wang. Coke formation during thermal treatment of bio-oil. *Energy and Fuels*, 34:7863–7914, 7 2020.

[44] Dan Liu, Gaofeng Li, Feifei Yang, Hua Wang, Jinyu Han, Xinli Zhu, and Qingfeng Ge. Competition and cooperation of hydrogenation and deoxygenation reactions during hydrodeoxygenation of phenol on pt(111). *Journal of Physical Chemistry C*, 121:12249–12260, 6 2017.

[45] João Lourenço Castagnari Willimann Pimenta, Mariana de Oliveira Camargo, Rafael Belo Duarte, Onelia Aparecida Andreo dos Santos, and Luiz Mario de Matos Jorge. Deoxygenation of vegetable oils for the production of renewable diesel: Improved aerogel based catalysts. *Fuel*, 290, 4 2021.

[46] Elham Nejadmoghadam, Abdenour Achour, Pouya Sirous-Rezaei, Muhammad Abdus Salam, Prakhar Arora, Olov Öhrman, Derek Creaser, and Louise Olsson. Stabilization of bio-oil from simulated pyrolysis oil using sulfided nimo/al2o3 catalyst. *Fuel*, 353, 12 2023.

[47] Niklas Bergvall, You Wayne Cheah, Christian Bernlind, Alexandra Bernlind, Louise Olsson, Derek Creaser, Linda Sandström, and Olov G.W. Öhrman. Upgrading of fast pyrolysis bio-oils to renewable hydrocarbons using slurry- and fixed bed hydroprocessing. *Fuel Processing Technology*, 253, 1 2024.

[48] Shinyoung Oh, Jae Hoon Lee, and Joon Weon Choi. Hydrodeoxygenation of crude bio-oil with various metal catalysts in a continuous-flow reactor and evaluation of emulsion properties of upgraded bio-oil with petroleum fuel. *Renewable Energy*, 160:1160–1167, 11 2020.

[49] Edward Furimsky. Catalytic hydrodeoxygenation. Technical report, 2000.

[50] Mariefel V. Olarte, Alan H. Zacher, Asanga B. Padmaperuma, Sarah D. Burton, Heather M. Job, Teresa L. Lemmon, Marie S. Swita, Leslie J. Rotness, Gary N. Neuenschwander, John G. Frye, and Douglas C. Elliott. Stabilization of softwood-derived pyrolysis oils for continuous bio-oil hydroprocessing. *Topics in Catalysis*, 59:55–64, 1 2016.

[51] Andrey Popov, Elena Kondratieva, Laurence Mariey, Jean Michel Goupil, Jaafar El Fallah, Jean Pierre Gilson, Arnaud Travert, and Françoise Maugé. Bio-

oil hydrodeoxygenation: Adsorption of phenolic compounds on sulfided (co)mo catalysts. *Journal of Catalysis*, 297:176–186, 1 2013.

[52] Oliver M. Daniel, Andrew Delariva, Edward L. Kunkes, Abhaya K. Datye, James A. Dumesic, and Robert J. Davis. X-ray absorption spectroscopy of bimetallic pt-re catalysts for hydrogenolysis of glycerol to propanediols. *ChemCatChem*, 2:1107–1114, 9 2010.

[53] Sri Kadarwati, Xun Hu, Richard Gunawan, Roel Westerhof, Mortaza Gholizadeh, M. D.Mahmudul Hasan, and Chun Zhu Li. Coke formation during the hydrotreatment of bio-oil using nimo and como catalysts. *Fuel Processing Technology*, 155:261–268, 1 2017.

[54] Tatiana Bochko and Andrey Shishov. The effect of hydrotreating on the pyrolysis oil composition by gc-ms. *Analytical Methods*, 2026.

[55] Isah Yakub Mohammed, Feroz Kabir Kazi, Yousif Abdalla Abakr, Suzana Yusuf, and Md Abdur Razzaque. Novel method for the determination of water content and higher heating value of pyrolysis oil. Technical report.

[56] Charles A. Mullen, Gary D. Strahan, and Akwasi A. Boateng. Characterization of biomass pyrolysis oils by diffusion ordered nmr spectroscopy. *ACS Sustainable Chemistry and Engineering*, 7:19951–19960, 12 2019.

[57] Naijia Hao, Haoxi Ben, Chang Geun Yoo, Sushil Adhikari, and Arthur J. Ragauskas. Review of nmr characterization of pyrolysis oils, 9 2016.

[58] A. Skreiberg, O. Skreiberg, J. Sandquist, and L. Sørum. Tga and macro-tga characterisation of biomass fuels and fuel mixtures. *Fuel*, 90:2182–2197, 6 2011.

[59] Elham Nejadmoghadam, Olov Öhrman, Derek Creaser, and Louise Olsson. Impact of dewatering on pyrolysis oil upgrading: A comparative study of properties and hydrodeoxygenation. *Chemical Engineering Journal*, 533, 4 2026.

[60] Jan J. Wiesfeld, Minjune Kim, Kiyotaka Nakajima, and Emiel J.M. Hensen. Selective hydrogenation of 5-hydroxymethylfurfural and its acetal with 1,3-propanediol to 2,5-bis(hydroxymethyl)furan using supported rhenium-promoted nickel catalysts in water. *Green Chemistry*, 22:1229–1238, 2 2020.

[61] Martin Staš, Miloš Auersvald, Lukáš Kejla, Dan Vrtiška, Jiří Kroufek, and David Kubička. Quantitative analysis of pyrolysis bio-oils: A review, 5 2020.

A

Appendix A

Table A.1: GC-MS chromatograms of the PO feedstock, showing the identified compounds along with their names and chemical formulas.

Classification	Compound in PO Feedstock	Formula
Acids	1-Pyridineacetic acid, hexahydro-	C7H13NO2
	3-Isopropoxy alanine	C6H13NO3
	4-Hexenoic acid, 4-methyl-6-(fluorodimethylsilyl)-6-trimethylsilyl-	C12H25FO2Si2
	5,8,11-Eicosatrienoic acid, (Z)-	C23H42O2Si
	9,12-Octadecadienoic acid (Z,Z)-	C21H40O2Si
	Acetic acid	C2H4O2
	Ala-ß-Ala, N-trimethylsilyl-, trimethylsilyl ester	C12H28N2O3Si2
	Benzoic acid, 3,4,5-trimethoxy-2-nitro-	C10H11NO7
	D-tert-Leucine	C6H13NO2
	Dehydroabietic acid	C23H36O2Si
	dl-2-Aminocaprylic acid	C8H17NO2
	dl-Leucine, N-[(phenylmethoxy)carbonyl]-	C14H19NO4
	Dodecanoic acid	C18H38O2Si
	Eicosapentaenoic Acid	C23H38O2Si
	Glycine	C2H5NO2
	Pimaric acid	C20H30O2
	trans-2-undecenoic acid	C11H20O2
Sugars	2,3-Anhydro-d-mannosan	C6H8O4
	2,7-Anhydro-l-galacto-heptulofuranose	C7H12O6
	2'-Desoxyuridine	C15H28N2O5Si2
	5-O-Methyl-d-gluconic acid dimethylamide	C9H19NO6
	6-Acetyl-ß-d-mannose	C8H14O7
	D-Allose	C6H12O6
	Melezitose	C18H32O16
	Methyl 4-O-acetyl-2,3,6-tri-O-ethyl-α-d-galactopyranoside	C15H28O7
	ß-D-Glucopyranose, 1,6-anhydro-	C6H10O5
	ß-D-Xylofuranose, 1,2-bis-O-(trimethylsilyl)-, cyclic methylboronate	C12H27BO5Si2
	Vanillin lactoside	C20H28O13
	α-D-Galactopyranose, 6-O-(trimethylsilyl)-, cyclic 1,2:3,4-bis(methylboronate)	C11H22B2O6Si
	α-D-Galactopyranoside, methyl 2-(acetylamino)-2-deoxy-3,4-di-O-methyl-6-O-(trimethylsilyl)-	C14H29NO6Si
	α-D-Glucopyranose, 4-O-ß-D-galactopyranosyl-	C12H22O11
	α-D-Glucopyranoside, methyl 2-(acetylamino)-2-deoxy-3-O-(trimethylsilyl)-, cyclic methylboronate	C13H26BNO6Si
	α-D-Mannopyranose, 1-O-(trimethylsilyl)-, cyclic 2,3:4,6-bis(methylboronate)	C11H22B2O6Si
	α-D-Xylofuranoside, methyl 5-O-methyl-	C7H14O5
	α-l-Galactopyranoside, methyl 6-deoxy-2-O-(trimethylsilyl)-, cyclic butylboronate	C14H29BO5Si

Furans	2-Furancarboxylic acid, 2-methoxyethyl ester	C8H10O4
	2-Furanone, 2,5-dihydro-3,5-dimethyl	C6H8O2
	2-Furanpropanoic acid	C10H16O3Si
	3-Furaldehyde	C5H4O2
	3-Methyl-2-furoic acid	C9H14O3Si
	5-Hydroxymethylfurfural	C6H6O3
	Furfuryl alcohol	C8H14O2Si

Ketones & Aldehydes	1-Methyl-4-amino-4,5(1H)-dihydro-1,2,4-triazole-5-one	C3H6N4O
	(1R,4aR,4bS,7S,10aR)-1,4a,7-Trimethyl-7-vinyl-1,2,3,4,4a,4b,5,6,7,8,10,10a- dodecahydrophenanthrene-1-carbaldehyde	C20H30O
	1-Penten-3-one	C5H8O
	1-Penten-3-one, 2-methyl-	C6H10O
	1-Phenyl-2-propanone	C9H10O
	1,2-Cyclopentanedione, 3-methyl-	C6H8O2
	1,2-Hydrazinedicarboxamide	C2H6N4O2
	2-Butenal, 2-methyl-	C5H8O
	2-Hexenal, 2-ethyl-	C8H14O
	2-Pentenal, 2-methyl-	C6H10O
	2,2-Dimethyl-5-[2-(2-trimethylsilylethoxymethoxy)-propyl]-[1,3]dioxolane-4-carboxaldehyde	C15H30O5Si
	2,3-Pentanedione	C5H8O2
	2(1H)-Naphthalenone, 1-(dimethoxymethyl)-3,4,5,6,7,8-hexahydro-	C13H20O3
	3-Heptyne-2,6-dione, 5-methyl-5-(1-methylethyl)-	C11H16O2
	3-Methylcyclopentane-1,2-dione	C6H8O2
	3-Penten-2-one, (E)-	C5H8O
	3-Penten-2-one, 3-methyl-	C6H10O
	4-Hexenal, 3-(t-butyldimethylsilyloxy)-	C12H24O2Si
	5,9-Dodecadien-2-one, 6,10-dimethyl-, (E,E))-	C14H24O
	7-Octen-4-one, 2,6-dimethyl-	C10H18O
	7,9-Diethyl-2,4-bis(dimethylamino)-10-imino-8-thio-1,7,9-triazaspiro[4.5]-1,3-decadiene-6,8-dione	C15H24N6OS
	Decanal	C10H20O
	Methacrolein	C4H6O
	Succindialdehyde	C4H6O2

Esters & Ethers	1,2-Dimethyl-6-(2-trimethylsilylethoxymethoxy) cyclohexanecarboxylic acid, methyl ester	C16H32O4Si
	1-(4-Methoxyphenyl)piperazine	C14H24N2OSi
	1-Butyne, 4,4-dimethoxy-	C6H10O2
	1-Methoxy-4-nitro-2,3,5,6-tetramethylbenzene	C11H15NO3
	1-Methyl-1-(2-tetrahydrofurylmethoxy)-1-silacyclopentane	C10H20O2Si
	1,1-Dimethylethanol	C7H18OSi
	2-[2-[2-[2-(2-Butoxyethoxy)ethoxy]ethoxy]ethoxy]ethyl acetate	C16H32O7
	2-Ethoxytetrahydrofuran	C6H12O2
	2-Ethylbutyl acrylate	C9H16O2
	2-Oxiranecarboxylic acid, 3-(2,2-dimethoxyethyl)-3-methyl-, methyl ester	C9H16O5
	2-Oxiranemethanol, α-(1-methylethyl)-3-[1-(trimethylsilyloxy)pentyl]-	C14H30O3Si
	2-Propenoic acid, 4-methylpentyl ester	C9H16O2
	3-(Decyloxy)-2-[(trimethylsilyl)oxy]propan-1-amine	C16H37NO2Si
	3-Oxatricyclo[3.2.1.0(2,4)]Octane-6-carboxylic acid, 8-(trimethylsilyl)-, methyl ester	C12H20O3Si
	3,4-Dimethoxytoluene	C9H12O2
	5-Keto-2,2-dimethylheptanoic acid, ethyl(ester)	C11H20O3
	6-Ethyl-3-dimethyl(isopropyl)oxydecane	C17H38OSi
	Acetic acid, 2-ethylbutyl ester	C8H16O2
	Bicyclo[2.2.1]heptan-2-ol, 7,7-dimethyl-, acetate	C11H18O2
	Butanoic acid, 3-methyl-, 5-methyl-2-(1-methylethyl)cyclohexyl ester, (1α,2ß,5α)-	C15H28O2
	Carbamic acid, (3,4,4-trimethyl-1,2-dioxetan-3-yl)methyl ester	C7H13NO4
	Carbamic acid, methyl ester	C2H5NO2
	Crotonic acid	C10H20O2Si
	Dodecanoic acid, 2,3-bis(acetyloxy)propyl ester	C19H34O6
	E-9-Methyl-8-tridecen-2-ol, acetate	C16H30O2
	Ethanol, 2-nitro-, propionate (ester)	C5H9NO4
	Ethylene glycol	C5H14O2Si
	Ethyltriethylene glycol	C14H32O4Si
	Formic acid	C7H16O2Si
	Glycolic acid	C8H20O3Si2
	Heptane, 1,1-dimethoxy-	C9H20O2
	Hexane, 1-(1-ethoxyethoxy)-	C10H22O2
	Isobutanol	C7H18OSi
	Methyl abietate	C21H32O2
	Propane, 1,1-dimethoxy-	C5H12O2
	Propane, 2,2'-[ethylidenebis(oxy)]bis-	C8H18O2
	Propane, 2,2'-[methylenebis(oxy)]bis-	C7H16O2
	Propane, 2,2',2''-[methylidynetris(oxy)]tris-	C10H22O3
	Propanoic acid, 2-oxo-, ethyl ester	C5H8O3
	Silane, [3-(2,3-epoxypropoxy)propyl]ethoxydimethyl-	C10H22O3Si
	Silane, trimethyl(propoxymethyl)-	C7H18OSi

Alcohols	1-Cyclopentylethanol	C10H22OSi
	1-Hexanol, 2,2-dimethyl-	C8H18O
	1-Tridecanol	C16H36OSi
	1,2,3-Butanetriol	C4H10O3
	1,3-Octanediol	C8H18O2
	2-Furanol, tetrahydro-2,3-dimethyl-, trans-	C6H12O2
	2-Propanol, 1-amino-, (R)-	C3H9NO
	2,3-Butanediol	C4H10O2
	3-(Decyloxy)-2-[(trimethylsilyl)oxy]propan-1-amine	C16H37NO2Si
	3-Ethyl-4-methyl-3-heptanol	C10H22O
	3-Hexanol, 3,4-diethyl-,	C10H22O
	3-Octen-2-ol, (E)-	C11H24OSi
	3-Pentyn-1-ol, 2-[(trimethylsilyl)ethynyl]-	C10H16OSi
	5-Dimethyl(isopropyl)silyloxytridecane	C18H40OSi
	5-Hepten-3-yn-2-ol, 6-methyl-5-(1-methylethyl)-	C11H18O
	Benzenemethanol, α,α-dimethyl-	C9H12O
	Ethanol, 2-(trimethylsilyl)-	C5H14OSi
	exo-Norbornanol, allyldimethylsilyl ether	C12H22OSi
	Silanol, trimethyl-	C3H10OSi

Phenols	2-Isopropoxyphenoxy	C12H20O2Si
	2-Methoxy-5-methylphenol	C8H10O2
	2-Methoxy-5-methylphenol	C11H18O2Si
	2-Propanone, 1-(4-hydroxy-3-methoxyphenyl)-	C10H12O3
	3-Allyl-6-methoxyphenol	C10H12O2
	4-((1E)-3-Hydroxy-1-propenyl)-2-methoxyphenol	C10H12O3
	Apocynin	C9H10O3
	Benzaldehyde, 3-hydroxy-4-methoxy-	C8H8O3
	Benzenepropanol, 4-hydroxy-3-methoxy-	C10H14O3
	Catechol	C9H14O2Si
	p-Cymene-2,5-diol	C10H14O2
	Phenol, 2-methoxy-	C7H8O2
	Phenol, 2-methoxy-4-(1-propenyl)-	C10H12O2
	Phenol, 2-methoxy-4-methyl-6-[propenyl]-	C11H14O2
	Phenol, 2-methoxy-4-propyl-	C10H14O2
	Phenol, 2-methoxy-5-(1-propenyl)-, (E)-	C10H12O2
	Phenol, 4-(3-hydroxy-1-propenyl)-2-methoxy-	C10H12O3
	Phenol, 4-ethyl-2-methoxy-	C9H12O2
	Phenylacetylformic acid, 4-hydroxy-3-methoxy-	C10H10O5
	Resorcinol	C9H14O2Si
	Silane, trimethyl(4-phenoxybutoxy)-	C13H22O2Si
	Vanillin	C8H8O3
	α-Tetralol, 2-amino-5,6-dimethoxy-	C12H17NO3

Multiple Oxygenates	(S)-(-)-1,2,4-Butanetriol, 2-acetate	C6H12O4
	1-Buten-3-one, 1-(2-carboxy-4,4-dimethylcyclobutenyl)-	C11H14O3
	1,2-Butanediol, 1-(2-furyl)-2-methyl-	C9H14O3
	1,2-Propanediol, 1-acetate	C5H10O3
	1,2-Propanediol, 2-acetate	C5H10O3
	2-Butanone, 4-hydroxy-3-(hydroxymethyl)-3-methyl-	C6H12O3
	2-Cyclopenten-1-one, 2-hydroxy-	C5H6O2
	2-Propanol, 1-(1-methylethoxy)-	C6H14O2
	2-Propanone, 1-(acetyloxy)-	C5H8O3
	2-Propanone, 1-hydroxy-	C3H6O2
	2,2-Dimethyl-5-[2-(2-trimethylsilylethoxymethoxy)-propyl]-[1,3]dioxolane-4-carboxaldehyde	C15H30O5Si
	2,3-Butanediol, dinitrate	C4H8N2O6
	2(1H)-Naphthalenone, 1-(dimethoxymethyl)-3,4,5,6,7,8-hexahydro-	C13H20O3
	3-(1-Ethoxy-ethoxy)-butan-1-ol	C8H18O3
	3,3-Diethoxy-1-propanol	C7H16O3
	9-Oxabicyclo[3.3.1]nonan-2-one, 3-methyl-6-(tetrahydro-2H-2-pyranyloxy)-	C14H22O4
	Acetic acid, (acetyloxy)-	C4H6O4
	Acetic acid, dimethoxy-, methyl ester	C5H10O4
	Carbophenoxon sulfone	C11H16ClO5PS2
	Diethoxymethyl acetate	C7H14O4
	Ethyl N-hydroxyacetimidate	C4H9NO2
	Propanoic acid, 2-hydroxy-, ethyl ester	C5H10O3
	TATP	C9H18O6

Non-oxygenated Compounds	1,2,4,5-Tetrazine	C2H2N4
	Ethanethioamide	C2H5NS
	Hydrazine, 1,2-dimethyl-	C2H8N2
	Pentane, 2-bromo-2-methyl-	C6H13Br
	Retene	C18H18
	Silane, bicyclo[2.2.1]hept-2-en-2-yltrimethyl-	C10H18Si
	Formamide, N-methylthio	C2H5NS

Table A.2: GC-MS chromatograms of the PO HDO product, showing the identified compounds along with their names and chemical formulas.

Classification	Compounds after HDO of PO	Formula
Alcohols	1-Pentanol	C5H12O
Furans	2H-Pyran-2-one, tetrahydro-6-methyl-	C6H10O2
Aldehydes & Ketones	2,4-Azetidinedione, 3,3-diethyl-1-methyl-	C8H13NO2
	2,2,4-Trimethyl-3-pentanone	C8H16O
	2-Piperidinone, N-[4-bromo-n-butyl]-	C9H16BrNO
	Propanal, 2,2-dimethyl-	C5H10O
Esters & Ethers	5-Ethoxy-2-phenyl-4,5-dihydrooxazol	C11H13NO2
	Sulfurous acid, butyl decyl ester	C14H30O3S
Multiple Oxygenates	Benzyl 2-chloroethyl sulfone	C9H11ClO2S
HC	1-Octene, 6-methyl-	C9H18
	1,7-Dimethyl-4-(1-methylethyl)cyclodecane	C15H30
	1H-Indene, 1-ethyl-2,3-dihydro-1-methyl-	C12H16
	2-Hexene, 2,3-dimethyl-	C8H16
	2-Hexene, 3,4,4-trimethyl-	C9H18
	3-Hexene, 2,2-dimethyl-, (Z)-	C8H16
	3-Hexene, 3-ethyl-2,5-dimethyl-	C10H20
	3,5-Dimethyl-3-heptene	C9H18
	4-Chloro-2,4-dimethylhexane	C8H17Cl
	Benzene, (1-cyclopropyl-1-methylethyl)-	C12H16
	Benzene, 1-ethenyl-4-ethyl-	C10H12
	Benzene, 1-ethyl-2-methyl-	C9H12
	Benzene, 1-ethyl-4-(1-methylethyl)-	C11H16
	Benzene, 1,4-diethyl-	C10H14
	Benzene, propyl-	C9H12
	Cyclohexane	C6H12
	Cyclohexane, (1-methylpropyl)-	C10H20
	Cyclohexane, 1-methyl-3-(1-methylethenyl)-, cis-	C10H18
	Cyclohexane, 1,2,3-trimethyl-, (1α,2α,3ß)-	C9H18
	Cyclohexane, 1,3-dimethyl-, cis-	C8H16
	Cyclohexane, pentyl-	C11H22
	Cyclopentane, 1,3-dimethyl-	C7H14
	Cyclopentane, methyl-	C6H12
	Decane, 5-propyl-	C13H28
	Ethylbenzene	C8H10
	Heptane, 2,4-dimethyl-	C9H20
	Heptane, 3-methyl-	C8H18
	Heptane, 3,4,5-trimethyl-	C10H22
	Hexane, 2,3,4-trimethyl-	C9H20
	Hexane, 3-methyl-	C7H16
	m-Menthane, (1S,3S)-(+)-	C10H20
	Naphthalene, 1,2,3,4-tetrahydro-6-methyl-	C11H14
	Nonane, 5-(2-methylpropyl)-	C13H28
	Octadecane, 1-iodo-	C18H37I
	Pentane, 2-methyl-	C6H14
	Pentane, 2,2,3,3-tetramethyl-	C9H20
	Pentane, 3-ethyl-2,2-dimethyl-	C9H20
	Pentane, 3-methyl-	C6H14
	Undecane, 2,4-dimethyl-	C13H28
	Undecane, 5-methyl-	C12H26

Table A.3: GC-MS chromatograms of the BO feedstock, showing the identified compounds along with their names and chemical formulas.

Classification	Compound in BO Feedstock	Formula
Acids	9,12-Octadecadienoic acid (Z,Z)-	C21H40O2Si
	Dehydroabietic acid	C23H36O2Si
Esters & Ethers	6-Isopropyl-1-oxaspiro[2.5]octane-4,5-dicarboxylic acid, dimethyl ester	C14H22O5
	Butanedioic acid, 2-(1-methoxy-1-methylethoxy)-3-methyl-, diethyl ester, [S-(R*,S*)]-	C13H24O6
	Butanedioic acid, dibutyl ester	C12H22O4
	cis-9-Octadecenoic acid, propyl ester	C21H40O2
	Docosanoic acid, butyl ester	C26H52O2
	Eicosanoic acid, isobutyl ester	C24H48O2
	Formic acid, butyl ester	C5H10O2
	Hexadecanoic acid, butyl ester	C20H40O2
	n-Propyl acrylate	C6H10O2
	Nonanedioic acid, dibutyl ester	C17H32O4
	Oxetane, 2,3,4-trimethyl-, (2α,3α,4ß)-	C6H12O
Alcohols	1-Butanol	C4H10O
	Silanol, trimethyl-	C3H10OSi
Multiple Oxygenates	1-Butanamine, N-nitro-	C4H10N2O2
Non-oxygenated Compounds	Butane, 1-chloro-	C4H9Cl

Table A.4: GC-MS chromatograms of the BO HDO product, showing the identified compounds along with their names and chemical formulas.

Classification	Compounds after HDO of BO	Formula
Acids	5,8,11,14-Eicosatetraynoic acid	C20H24O2
	Pimaric acid	C20H30O2
Aldehydes & Ketones	1-Phenanthrenecarboxaldehyde, 1,2,3,4,4a,9,10,10a-octahydro-1,4a-dimethyl-7-(1-methylethyl)-, [1S-(1α,4aα,10aß)]-	C20H28O
	1H-Inden-1-one, 2-(2,3-dihydro-1H-inden-1-ylidene)-2,3-dihydro-	C18H14O
	2-Piperidinone, N-[4-bromo-n-butyl]-	C9H16BrNO
	2,2,4-Trimethyl-3-pentanone	C8H16O
	2,4-Azetidinedione, 3,3-diethyl-1-methyl-	C8H13NO2
	2,5,5-Trimethyl-3-phenyl-cyclohexanone	C15H20O
	3a,9b-Dimethyl-1,2,3a,4,5,9b-hexahydrocyclopenta[a]naphthalen-3-one	C15H18O
	Cycloheptanone, 4-acetyl-7,7-dimethyl-2-(2-oxopropyl)-	C14H22O3
	Propanal, 2,2-dimethyl-	C5H10O
	Tricyclo[8.4.1.1(3,8)]hexadeca-3,5,7,10,12,14-hexaen-2-one, anti-	C16H14O
	Tricyclo[8.4.1.1(3,8)]hexadeca-3,5,7,10,12,14-hexaene-2,9-dione, anti-	C16H12O2
Esters & Ethers	1-(2-Vinylphenyl)-1H-isochromene	C17H14O
	1-Phenanthrenecarboxylic acid, 1,2,3,4,4a,10a-hexahydro-1,4a-dimethyl-7-(1-methylethyl)-, methyl ester, [1R-(1α,4aß,10aα)]-	C21H28O2
	10-Chloro-1-decanol, pentafluoropropionate	C13H20ClF5O2
	1H-Indene, 2,3-dihydro-2-methoxy-1-phenyl-, cis-	C16H16O
	2,5-Octadecadiynoic acid, methyl ester	C19H30O2
	4-Benzyloxybenzonitrile	C14H11NO
	5,8,11-Heptadecatriynoic acid, methyl ester	C18H24O2
	9,12,15-Octadecatrienoic acid, 2-(acetyloxy)-1-[(acetyloxy)methyl]ethyl ester, (Z,Z,Z)-	C25H40O6
	Benzaldehyde, 4-(1-phenyl-2-propenyloxy)-	C16H14O2
	Benzeneacetic acid, 4-tridecyl ester	C21H34O2
	Benzo[b]furan, 3-(4-methoxyphenyl)-2,6-dimethyl-	C17H16O2
	Cyclopropane, 1-ethoxy-2,2-dimethyl-3-(2-phenylethenylidene)-	C15H18O
	Ethanol, 2-(tetradecyloxy)-	C16H34O2
	Geranyl isovalerate	C15H26O2
	Methanesulfonic acid, 7,8,9,10-tetrahydrocyclohepta[de]naphthalen-8-yl ester	C15H16O3S
	trans-Verbenyl laureate	C22H38O2
	Tricyclo[4.2.1.0(2,5)]nona-3,7-diene, 9-methoxy-1-phenyl-	C16H16O
Alcohols	1-Hexadecanol, 2-methyl-	C17H36O
	1-Pentanol, 4-methyl-	C6H14O
	1,2,2-Trimethyl-3-phenyl-cyclopent-3-enol	C14H18O
	4a,10a-Methanophenanthren-9ß-ol, 11-syn-bromo-1,2,3,4,4a,9,10,10a-octahydro-	C15H17BrO
	6-Octen-1-yn-3-ol, 3,7-dimethyl-	C10H16O
	9-Methyltricyclo[4.2.1.1(2,5)]deca-3,7-diene-9,10-diol	C11H14O2
	Anthracene, 9,10-dihydro-9-(2-hydroxy-2-propyl)-9,10-dimethyl-	C19H22O
	Ethanol, 1-(2,2-dimethyl-1-phenylethynylcyclopropyl)-	C15H18O
	Falcarinol	C17H24O
	Fluorene, 4-[1,2-dihydroxyethyl]-	C15H14O2
	Isocalamenediol	C15H26O2
	Tricyclo[7.4.1.1(2,7)]pentadeca-2,4,6,9,11,13-hexaene-8-ol	C15H14O
	α-N-Normethadol	C20H27NO
Phenols	4-Phenanthrenol, 1,2,3,4-tetrahydro-4-methyl-	C15H16O
	trans-10,11-Dihydro-11-methylbenz[a]anthracene-10,11-diol	C19H16O2
	trans-8,9-Dihydro-11-methylbenz(a)anthracene-8,9-diol	C19H16O2

Multiple Oxygenates	1-Oxaspiro[4.4]non-8-ene-4,7-dione, 9-hydroxy-6-(3-methyl-2-butenyl)-2-(1-methylethyl)-8-(3-methyl-1-oxobutyl)-	C21H30O5
	1,4-Bis(nitratomethyl)anthracene	C16H12N2O6
	14-Oxononadec-10-enoic acid, methyl ester	C20H36O3
	2-Dodecen-1-yl(-)succinic anhydride	C16H26O3
	5-[(2,4-Dinitrophenyl)-hydrazonomethyl]-dihydrofuran-2-one	C11H10N4O6
	5,7,9(11)-Androstatriene, 3-hydroxy-17-oxo-	C19H24O2
	Benzaldehyde, 3-benzyloxy-2-fluoro-4-methoxy-	C15H13FO3
	Benzyl 2-chloroethyl sulfone	C9H11ClO2S
	Butanoic acid, 3-[(1-phenylethyl-2-propynyl)oxy]	C15H18O3
	Cyclohexane-1-carboxylic acid, 3-[3-(2-furyl)-1-oxopropyl]-6,6-dimethyl-2,4-dioxo-, methyl ester	C17H24O6
	Phenanthrene-1-acetaldehyde, 7-acetoxy-2ß-cyano-2,4b-dimethyl-	C21H31NO3
	Pregnenolone-7,9(11)-dien	C21H28O2
	Propane, 2-nitro-	C3H7NO2

HC	(1,4-Dimethylpent-2-enyl)benzene	C13H18
	1-benzyl-3-methylnaphthalene	C18H16
	1-Chloroeicosane	C20H41Cl
	1-Isopropenylnaphthalene	C13H12
	1-Methyl-4-p-tolylnaphthalene	C18H16
	1-Pentene	C5H10
	1-Pentene, 2-methyl-	C6H12
	1,1'-Biphenyl, 2,2',5,5'-tetramethyl-	C16H18
	1,1'-Biphenyl, 2,4'-dimethyl-	C14H14
	1,1'-Biphenyl, 3,4-diethyl-	C16H18
	1,1'-Biphenyl, 4-(1-methylethyl)-	C15H16
	1,3-Cyclohexadiene, 2,6,6-trimethyl-1-(3-methyl-1,3-butadienyl)-	C14H20
	1,3,8-p-Menthatriene	C10H14
	1,7-Dimethyl-3-phenyltricyclo[4.1.0.0(2,7)]hept-3-ene	C15H16
	1,8,15,22-Tricosatetrayne	C23H32
	10,11-Dihydro-5H-dibenzo(a,d)cycloheptene	C15H14
	1H-Cyclopropa[a]naphthalene, 1a,2,6,7,7a,7b-hexahydro-1,1,7,7a-tetramethyl-, [1aR-(1aα,7α,7aα,7bα)]-	C15H22
	1H-Indene, 1-ethylidene-	C11H10
	1H-Indene, 2,3-dihydro-1,1-dimethyl-	C11H14
	1H-Indene, octahydro-, trans-	C9H16
	2,2-Dimethylindene, 2,3-dihydro-	C11H14
	2,2,9,9-Tetramethyldec-5-ene-3,7-diyne	C14H20
	2,2'-Dimethylbiphenyl	C14H14
	3-Hexene, 3-ethyl-2,5-dimethyl-	C10H20
	3,5-Dimethyl-3-heptene	C9H18
	4H-Benz[de]anthracene, 5,6-dihydro-	C17H14
	7-Isopropyl-1,1,4a-trimethyl-1,2,3,4,4a,9,10,10a-octahydrophenanthrene	C20H30
	7-Methyl-7-(1-methylethenyl)-2-phenylbicyclo[4.2.0]oct-1-ene	C18H22
	8-Isopropyl-1,3-dimethylphenanthrene	C19H20
	9-Ethyl-10-methylanthracene	C17H16
	9H-Fluorene, 9,9-dimethyl-	C15H14
	Anthracene, 1,2,3,4-tetrahydro-	C14H14
	Anthracene, 9-ethyl-1,2,3,4,5,6,7,8-octahydro-	C16H22
	Azulene	C10H8
	Benzene	C6H6
	Benzene, (1-methylethyl)-	C9H12
	Benzene, (1-methylpropyl)-	C10H14
	Benzene, (1,1-dimethyl-2-propenyl)-	C11H14
	Benzene, (3-methyl-2-butenyl)-	C11H14
	Benzene, (4,5,5-trimethyl-1,3-cyclopentadien-1-yl)-	C14H16
	Benzene, 1-ethyl-4-methyl-	C9H12
	Benzene, 1-methyl-3-propyl-	C10H14
	Benzene, 1,2-diethyl-	C10H14
	Benzene, 1,2,3-trimethyl-	C9H12
	Bismuthine, trimethyl-	C3H9Bi

	Cyclodecacyclotetradecene, 14,15-didehydro-1,4,5,8,9,10,11,12,13,16,17,18,19,20-tetradecahydro-	C22H32
	Cyclohexane	C6H12
	Cyclohexane, 1,2-dimethyl-, trans-	C8H16
	Cyclohexane, 1,2,4-trimethyl-	C9H18
	Cyclohexene, 1-(1-propynyl)-	C9H12
	Cycloisolongifolene, 8,9-dehydro-9-vinyl-	C17H24
	Cyclopentane, (4-octyldodecyl)-	C25H50
	Cyclopentane, 1,3-dimethyl-, trans-	C7H14
	Cyclopentane, methyl-	C6H12
	Dibenzo[a,c]cyclooctene, 5,6,7,8-tetrahydro-	C16H16
	Ethylbenzene	C8H10
	Fluorene, 2,4a-dihydro-	C13H12
	Hept-2-ene, 2,4,4,6-tetramethyl-	C11H22
	Hexane, 2,3,4-trimethyl-	C9H20
	Indan, 1-methyl-	C10H12
	Naphthalene, 1-(2-propenyl)-	C13H12
	Naphthalene, 1,2-dimethyl-	C12H12
	Naphthalene, 1,2,3,4-tetrahydro-	C10H12
	Naphthalene, 1,2,3,4-tetrahydro-1-methyl-8-(1-methylethyl)-	C14H20
	Naphthalene, 1,2,3,4-tetrahydro-1,1,6-trimethyl-	C13H18
	Naphthalene, 1,2,3,4-tetrahydro-6-(1-phenylethyl)-	C18H20
	Naphthalene, 1,2,3,4-tetrahydro-6-methyl-	C11H14
	Naphthalene, 1,3-dimethyl-	C12H12
	Naphthalene, 1,6-dimethyl-4-(1-methylethyl)-	C15H18
	Naphthalene, 2-ethyl-	C12H12
	Naphthalene, 2,3-dimethyl-	C12H12
	Naphtho[3,4:2,3]bornene	C18H20
	Octadecane, 3-ethyl-5-(2-ethylbutyl)-	C26H54
	p-Cymene	C10H14
	Pentane, 2-methyl-	C6H14
	Pentane, 3-ethyl-2-methyl-	C8H18
	Pentane, 3-methyl-	C6H14
	Phenanthrene, 2-methyl-	C15H12
	Phenanthrene, 2,3-dimethyl-	C16H14
	Pyrene, 1,3-dimethyl-	C18H14
	Retene	C18H18
	s-Indacene, 1,2,3,5,6,7-hexahydro-1,1,4,8-tetramethyl-	C16H22
	Spiro[androstane-3,2'-thiazolidine], (5α)-	C21H35NS
	tert-Hexadecanethiol	C16H34S
	trans-4,4-Dimethyl-2-hexene	C8H16

DEPARTMENT OF SOME SUBJECT OR TECHNOLOGY
CHALMERS UNIVERSITY OF TECHNOLOGY
Gothenburg, Sweden
www.chalmers.se

CHALMERS
UNIVERSITY OF TECHNOLOGY